CHARACTERISATION AND PROPERTIES OF CALCIUM PHOSPHATE BIOCERAMIC DERIVED FROM ANIMAL BONES

LOO ZI ZHEN

FACULTY OF ENGINEERING
UNIVERSITY OF MALAYA
KUALA LUMPUR

2018

CHARACTERISATION AND PROPERTIES OF CALCIUM PHOSPHATE BIOCERAMIC DERIVED FROM ANIMAL BONES

LOO ZI ZHEN

DISSERTATION SUBMITTED IN FULFILMENT OF THE REQUIREMENTS FOR THE DEGREE OF MASTER OF ENGINEERING SCIENCE

FACULTY OF ENGINEERING
UNIVERSITY OF MALAYA
KUALA LUMPUR

2018

UNIVERSITY OF MALAYA

ORIGINAL LITERARY WORK DECLARATION

Name of Candidate: Loo Zi Zhen

Matric No: KGA140055

Name of Degree: Master of Engineering Science

Title of Project Paper/Research Report/Dissertation/Thesis ("this Work"):

Characterisation and properties of calcium phosphate bioceramic derived from animal bones

Field of Study: Advanced manufacturing

I do solemnly and sincerely declare that:

(1) I am the sole author/writer of this Work;
(2) This Work is original;
(3) Any use of any work in which copyright exists was done by way of fair dealing and for permitted purposes and any excerpt or extract from, or reference to or reproduction of any copyright work has been disclosed expressly and sufficiently and the title of the Work and its authorship have been acknowledged in this Work;
(4) I do not have any actual knowledge nor do I ought reasonably to know that the making of this work constitutes an infringement of any copyright work;
(5) I hereby assign all and every rights in the copyright to this Work to the University of Malaya ("UM"), who henceforth shall be owner of the copyright in this Work and that any reproduction or use in any form or by any means whatsoever is prohibited without the written consent of UM having been first had and obtained;
(6) I am fully aware that if in the course of making this Work I have infringed any copyright whether intentionally or otherwise, I may be subject to legal action or any other action as may be determined by UM.

Candidate's Signature Date:

Subscribed and solemnly declared before,

Witness's Signature Date:

Name:

Designation:

CHARACTERISATION AND PROPERTIES OF CALCIUM PHOSPHATE BIOCERAMIC DERIVED FROM ANIMAL BONES

ABSTRACT

Hydroxyapatite is being considered for applications in biomedical mainly due to its calcium to phosphorus ratio being similar to that of hard tissues, possessed excellent biocompatibility and exhibited superior osteoconduction characteristics. The synthesis of hydroxyapatite by using synthetic chemicals as the starting calcium precursors has been widely reported however the development of hydroxyapatite from using natural calcium source such as from bovine bones, eggshells, oyster shells, fish bones and corals are not systematically investigated as a potential resources for the production of high quality hydroxyapatite. In this work, the viability of preparing hydroxyapatite using natural available animal bones through a thermal decomposition method applied to bovine bone, caprine bone and galline bone have been investigated. The bone samples were sourced locally, cleaned to remove fats and proteins followed by calcination in an air atmosphere at different temperatures ranging from 600°C to 1000°C. The calcined powders were prepared and characterized to determine the phases present using X-ray diffraction and FTIR. The results revealed that the thermal stability of the HA matrix was not disrupted, particularly for the bovine bone and that all of the sintered bodies exhibited phase pure HA. This was not the case for the caprine and galline bones where a small amount of bioresorbable tri-calcium phosphate phase was observed after the calcination process. Nevertheless, bovine and caprine bone heat treated at 750°C and galline bone at 600°C were identified as the optimum calcination temperatures. Therefore heat treated powder at optimum temperatures was used to produce green bodies for the sintering process. The bulk density and mechanical properties of sintered samples were also measured.

Keywords: hydroxyapatite, animal bones, heat treatment, microstructure, phase analysis.

PENCIRIAN DAN SIFAT KALSIUM FOSFAT BIOSERAMIK YANG DIPEROLEHI DARIPADA TULANG HAIWAN

ABSTRAK

Hydroxyapatite banyak digunakan dalam aplikasi di bidang bioperubatan sebab nisbah kalsium dengan fosforus yang serupai dengan nisbah yang didapati pada tisu keras. Selain daripada itu, HA juga menunjukkan biocompatibility yang sangat baik dan atribut osteoconduction yang unggul. Sintesis HA yang menggunakan bahan kimia sebagai pendahulu kalsium telah banyak dilaporkan tetapi kekurangan laporan daripada yang menggunakan bahan kalsium semulajadi seperti tulang lembu, kulit telur, kulit tiram, tulang ikan serta batu karang. Bahan-bahan semulajadi ini harus disiasati potensi mereka sebagai bahan asas untuk menghasilkan HA yang berkualiti tinggi. Dalam pengajian ini, kesesuaian penghasilan HA menggukan kaedah penguraian haba pada tulang lembu, kambing dana yam telah disiasati. Sampel-sampel tulang didapati daripada sumber tempatan dan dibersihkan terutamanya lemak serta protein dan diterusi dengan proses calcination dalam keadaan atmosfera pada suhu 600°C sehingga ke 1000°C. Serbuk tulang yang telah diproses akan disediakan dan dicirikan untuk menuntukan fasa yang hadir dengan kaedah Difraksi Sinar-X dan Fourier-transform Infrared Spectroscopy. Keputusan menunjukkan struktur HA tidak diganggui dalam proses penguraian haba dan kestabilan terma HA kekal terutamanya pada sampel tulang lembu yang menunjukkan fasa HA tulen sahaja pada sampel yang dihasilkan pada semua peringkat suhu. Manakala pada sampel tulang kambing dan ayam, jumlah kecil fasa tri-kalsium fosfat yang boleh diserap oleh badan telah dijumpai. Sebagai kesimpulan, sampel tulang lembu dan kambing yang diproses pada tahap suhu 750°C dan sampel tulang ayam pada tahap suhu 600°C dikenal pasti sebagai suhu calcination yang paling optimum. Oleh itu, sebuk tulang yang dihasilkan daripada tahap suhu tertentu digunakan untuk menghasilkan sampel untuk proses sintering. Sampel yang dihasilkan daripada proses sintering adalah untuk menentukan ciri-ciri mekanikal serta ketumpatan pukal.

Keywords: hydroxyapatite, animal bones, heat treatment, microstructure, phase analysis.

ACKNOWLEDGEMENTS

Firstly, I would like to thank Department of Mechanical Engineering, University of Malaya for giving me an opportunity to work on this project. Without the great support of knowledge that been taught to me, I would never be able to finish the project. The mix of theory and practical education did help me a lot.

I would also like to express my highest gratitude to my supervisors, Prof. Ir. Dr. Ramesh Singh and Assoc. Prof. Dr. Tan Chou Yong for guiding me throughout the whole project. A lot of assistance and comments were given to help me in making this project a success. Without the advices, professional guidance and supervision this project may not be able to be carried out smoothly within time period given.

On top of that, I would like to thank the academians who gave me useful suggestions to make this a project a better one. I sincerely appreciate those valuable opinions and knowledge sharing. With just all the theory part, I could never be enough to finish this project. I would like to take this chance to thank staffs from laboratories. They gave me a lot of guidance and advices on the hands on to complete my study.

Lastly, I would like to thank my family for giving me continuous support throughout the years of my study. Also, I would like to thank my beloved friends who have been giving their support and assistance on parts that I am weaker at.

TABLE OF CONTENTS

LIST OF FIGURES

LIST OF TABLES

LIST OF SYMBOLS AND ABBREVIATIONS

Å	Angstrom
BMP	Bone morphogenetic proteins
Ca	Calcium
DCPA	Dicalcium phosphate anhydrous
DCPD	Dicalcium phosphate dehydrate
FGF	Fibroblast growth factor
FGF-23	Fibroblast growth factor-23
FTIR	Fourier transform infrared spectroscopy
GPa	Gigapascal
H	Hydrogen
HA	Hydroxyapatite
IGF	Insulin-like growth factor
ISO	International standard organization
JCPDS	Joint Committee on Powder Diffraction Standards
K	Potassium
Mg	Magnesium
mmol g^{-1}	Milimole per gram
MPa	Megapascal
Na	Sodium
nm	Nanometer
O	Oxygen
OCP	Octacalcium phosphate
P	Phosphorus
PDGF	Platelet-derived growth factor
SEM	Scanning electron microscope
SiC	Silicon cabide
TEM	Transmission electron microscopy
TGA	Thermo gravimetric analysis
TGF-β	Transforming growth factor-beta
Ti	Titanium
TTCP	Tetracalcium phosphate
UTS	Ultimate tensile stress
VEGF	Vascular endothelial growth factor
XRD	X-ray diffraction
YM	Young's modulus
α	Alpha
α-TCP	α-Tricalcium phosphate
β	Beta
β-TCP	β-Tricalcium phosphate
γ	Gamma
μm	Micrometer

LIST OF APPENDICES

CHAPTER 1: INTRODUCTION

1.1 Background study

The needs on biomaterials as implant is rising over the recent years. Taking bone grafting procedures as example, 10% of the substitutes used were of synthetic graft (Khan, Katti, & Laurencin, 2004). It is important to develop bone implants which are effective in assisting the healing process of large bone defects. The materials used must be having great bio-compatibility and non-toxicity so that the implants will not cause harm to patients (Yamada & Egusa, 2018). Autografts are currently being used widely but not only that the procedure is expensive, it may also be having the side effect of causing post-surgery complications (Ribeiro et al., 2018).

Biomaterials based on ceramics, polymers and composites were preferred over the metal counterparts due to various issues (Lin et al., 2017). Although metal part possess great mechanical properties but the stress shielding caused on bone will then weakens host tissue hence making it likely to fracture (Chen & Thouas, 2015). In the other hand, porous bio-ceramics provide a good medium that could promote healing of bone and subsequently form as a true bone tissues. Not only this technique would encourage faster healing, it would also eliminate the needs of repeated surgery at the healing site (Fuh, Huang, Chen, & Lin, 2017).

In the work of tissue engineering, hydroxyapatite (HA) was considered as one of the most efficient calcium phosphate to work on hence there was increasing demand in the usage of synthetic HA. The advantage of HA over other material was that it was able to control and lower the crystallinity (Zhang et al., 2018). Apart from that, HA was also

having great biological characteristics such as nontoxicity, lack of inflammatory and immunitary responses can be enhanced (Palazzo et al., 2007).

In recent works, there are HA derived from both natural and synthetic sources as well as through various processing routes. Due to the unique well organized way of the crystal formation of apatite in bone, there were difference between the biological and synthetic HA. The synthetic HA exhibited smaller crystal size hence having higher surface area (Danilchenko, Koropov, Protsenko, Sulkio-Cleff, & Sukhodub, 2006). This characteristics will allows the synthetic HA to adsorb more molecules (Palmer, Newcomb, Kaltz, Spoerke, & Stupp, 2008).

There were a handful of researcher working on the development of HA from natural sources. Currently developed natural source including bovine bone (Niakan et al., 2014), fish bone (Goto & Sasaki, 2014), porcine bone (Figueiredo et al., 2010), eggshells (Kamalanathan et al., 2014) and seashells (Rujitanapanich, Kumpapan, & Wanjanoi, 2014). Although there were many tested natural sources, bovine bone was the most well established sources due to the ease of obtaining and preparing samples as well as complying halal requirements.

Commonly in natural HA, there existed of carbonate ions as impurity as opposed to the synthetic HA. The carbonated ions found in natural HA appears to be an excellent material for bioresorbable bone substitutes (Suchanek et al., 2002). Characteristics of natural HA were highly depending on the method of extraction applied (Younesi, Javadpour, & Bahrololoom, 2011). In the case of biological apatites, it was found that

there are multiple substitutions as well as deficiencies at all ionic sites. Among all the compounds, it was important to highlight B-type carbonate HA which has carbonate substitution. In this compound, phosphate ions were substituted by carbonate (Leventouri, 2006).

1.2 Research problem statement

The study on heat treated bovine bone for natural porous HA was very well established but not in the case of caprine and galline bone (Mucalo, 2015). Moreover, the current available studies were focusing on the characterization or biological behaviour studies rather than improving the mechanical properties (Shi et al., 2018). It is discovered that there are more room to improve the mechanical properties of these HA by increasing the sintering temperature but most studies available only done up to 1000°C (Yetmez, Erkmen, Kalkandelen, Ficai, & Oktar, 2017). Apart from bovine bone, the other most studied bone is porcine bone but due to religious issue, it is important to discover more alternatives that are Halal compatible (Ofudje et al., 2018).

1.3 Goals and objectives of the study

1.3.1 Goals of the study

This study is aim to produce natural HA from raw animal bones which are bovine, caprine and galline. It is hope that HA with strong mechanical properties could be produced from the raw animal bones that collected as food waste. This does not only able to utilise waste material but also producing useful bio-ceramics at lower cost yet without the needs of using chemical. A good profile of characteristics and mechanical properties could be produced at the end of the study so that it would enable the production of HA with properties matching to each specific application. On top of all the improvement on

manufacturing processes, the raw bones were selected from reliable sources so that the HA produced meet halal standard.

1.3.2 Objectives of the study

The objectives of this study are listed as below;

- To identify the phase composition of HA derived from animal bones, specifically from bovine, caprine and galline
- To investigate the effects of sintering temperatures on the microstructure evolution and physical properties of the derived HA samples
- To evaluate the mechanical properties of the sintered samples through microhardness testing

1.4 Scope of the study

This study is limited to only certain specific areas of interest. Firstly, the source of bone chosen were only femur bone of bovine, caprine and galline. All the raw bones will be heat treated in two steps which are calcination and sintering. Secondly, both the heat treatment processes will be done only in conventional electric furnace under atmospheric condition. Thirdly, all specimens consist only pure crushed and sieved powder of calcined animal bones without any doping.

Characteristics of the produced specimens will be studied by X-ray diffraction (XRD) and Fourier transform infrared spectroscopy (FTIR). Scanning electron microscope (SEM) will be used to observer morphology of the sintered specimens. To study the mechanical properties, relative density and micro hardness were tested.

1.5 Structure of the dissertation

This dissertation started with chapter 1 with introduction on this research study. A brief idea on bio-materials and ceramics were explained in this chapter. Apart from that, it was also explained on the intention to carry out this study. Goals, objectives as well as scope of this study were stated in this chapter as well as guide and limit.

In chapter 2, literatures were studied and reviewed to make a comparison for what the current studies found and yet to discovered. Topics to review included general view on bone, brief overview on HA, natural sources of HA as well as the manufacturing processes employed. At the end of the chapter, a summary was done to conclude the findings so that it is easily to understand what have been done by other researchers.

Setup and planning of this study were explained in chapter 3. All the research procedures and plans were illustrated and explained. An overall timeline planning was made to guide the study to be done on time. From selection of raw materials to processing and then evaluation techniques used were explained here. Not only that to explain on certain steps and standard used but reason for chosen techniques also stated in here as reference for readers.

Chapter 4 is for the results presentation as well as discussion. All the data gathered will be analysed and discussed. Certain findings unique to this study will be further discussed and linked with current available studies to find the similarity and variance. The obtained results from XRD and FTIR show phase and chemical compound compositions found on the heat treated specimens. Each and every sintered specimens were also evaluated morphologically based on SEM micrographs obtained.

Finally, chapter 5 is a summary to this study. Conclusion made based on the results found within this study with recommendations for the future research work. Future research possibility including in vitro study on the cell growth and attachment onto the sintered specimens. Apart from that, other ways of heat treatment such as microwave and plasma sintering could be investigated.

CHAPTER 2: LITERATURE REVIEW

2.1 Bone

Mineralized hard tissues made up 206 bones in the body of adult humans which then form together as the endoskeleton of vertebrates (N. Umadevi & Dr. S.N. Geethalakshmi, 2011). Two major phases composed the bone which are organic and inorganic. Protein collagen formed the main part of organic phase while the phase of inorganic was dominated by hydroxyapatite (HA) and water. The three parts respectively accommodate 20%, 60% and 9% of the total mass of bone (R. Murugan & S. Ramakrishna, 2005). Functions of three different classes are found for bone which are mechanical, synthetic and metabolic. Shape of the body contributed by mechanical functions which also acts in protecting the internal organs as well as enabling various movement of body working together with muscles. Bone also carries synthetic function role which was to produce blood cells within the cavity of marrow. Apart from that two functions, bone also having important role in metabolic functions. Bone could act as storage of calcium and phosphate ions, buffering the blood as well as secreting osteocalcin and fibroblast growth factor-23 (FGF-23) which acting like an endocrine organ. Osteocalcin could increase secretion of insulin and sensitivity of cells to insulin to help in maintaining the concentration of blood sugar. FGF-23 in the other hand carrying the role on regulating kidneys to cease phosphate reabsorption.

Two different classes of bone structure were found in the adult skeleton system. Dense and low porosity (5-10%) tissue was known as the Cortical (compact) bone. Most of this tissue occurs in the shaft of long bones which they contributes to the mechanical properties of bone (J. A. Buckwalter, R. R. Cooper, M. J. Flimcher, & Recker, 1995). The other type of tissue was Cancellous (trabecular) bone which normally found in the ends

of long bones. It was a network of rod like and plate like elements with high porosity (30-90%) that inhabited by blood vessels and bone marrow. The architecture of bones is shown in Figure 2.1.

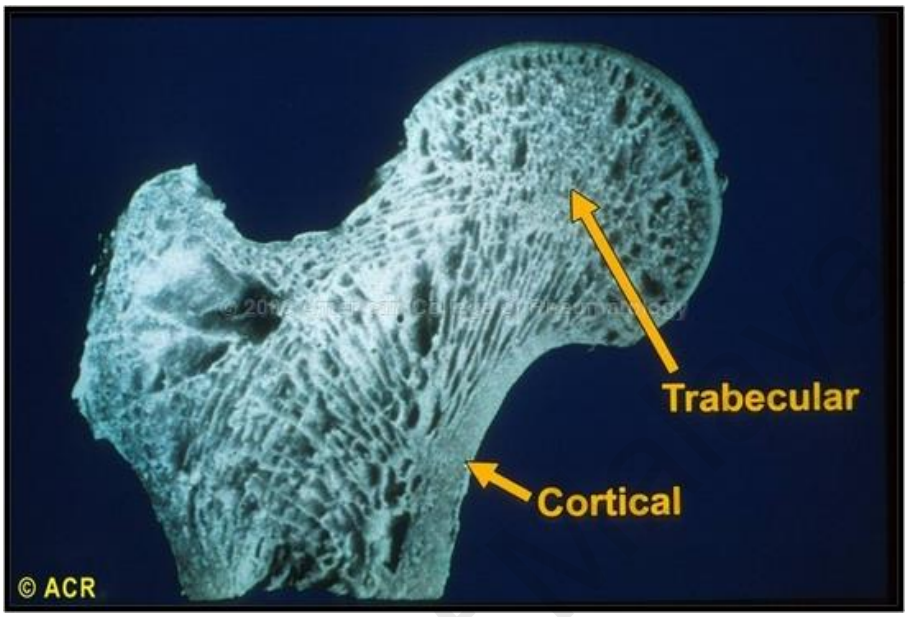

Figure 2.1: Bone Architecture (Rheumatology, 2009)

2.1.1 Physical characteristics of bone

Various levels of organizations of hierarchical structure made up the bone. The level and structures found are macrostructure, microstructure (10 to 500 μm), sub-microstructure (1 to 10 μm), nanostructure (100's nm to 1 μm) and sub-nanostructure. Cancellous and cortical bone were categorized under macrostructure. Under the microstructure, there were Haversian systems, osteons and single trabeculae while lamellae belongs to sub-microstructure. Categorized under nanostructure level were fibrillar collage and embedded mineral. Constituent elements found in the molecular structure, such as mineral, collagen and non-collagenous organic proteins were found in sub-nanostructure level. The arrangement of the hierarchically organized structure were

irregular but optimized. Orientation of the components made the bone heterogeneous and anisotropic (Sansalone et al., 2010).

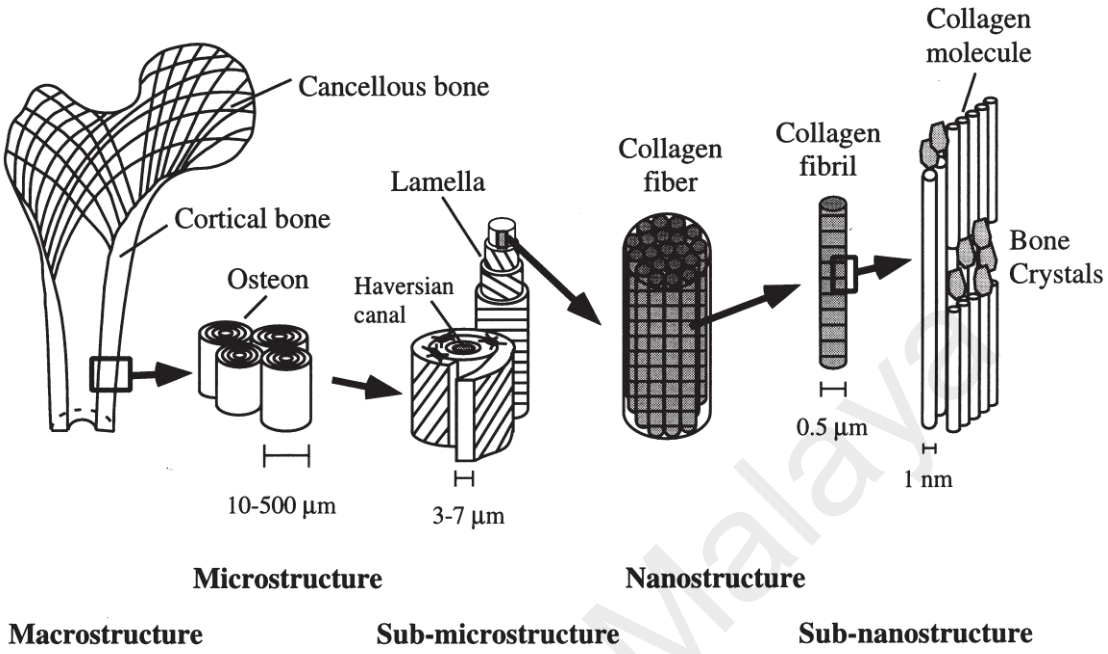

Figure 2.2: Hierarchical structural organization of bone *(Rho, Kuhn-Spearing, & Zioupos, 1998)*

Bone collagen was a fibrous molecule with length of 100nm to 2000nm. It was HA crystals that aligned longitudinally within the discrete spaces between collagen fibrils. The plate shaped crystals of HA are in the dimensions of 3 nm x 25 nm x 50 nm (Li & Aparicio, 2013). Though, doubts on the exact orientation of HA crystals in the relation to fiber of collage in still unclear. Danilchenko et al. studied in 2006 on the heating of both synthetic and natural sourced HA up to 500°C or 1300°C. The findings from X-ray diffraction patterns supported the prediction that rather than a continuous mineral phase with direct crystal-crystal bonding, the bone mineral is actually not a discrete aggregation of crystals.

Fiber of tropocollagen which was mainly composed of three intertwined polypeptides is the basic structural unit of collagen fibrils. Aminoacids, glycine, proline and hydroxyproline were the main polypeptides discovered. Steric forces caused by proline and hydroxyproline molecules held the polypeptides together. In contrast, the peptide bonds of α-helices where the peptide bonds are held together by hydrogen bonding (Gerhard Meisenberg & Willian H. Simmons, 2011).

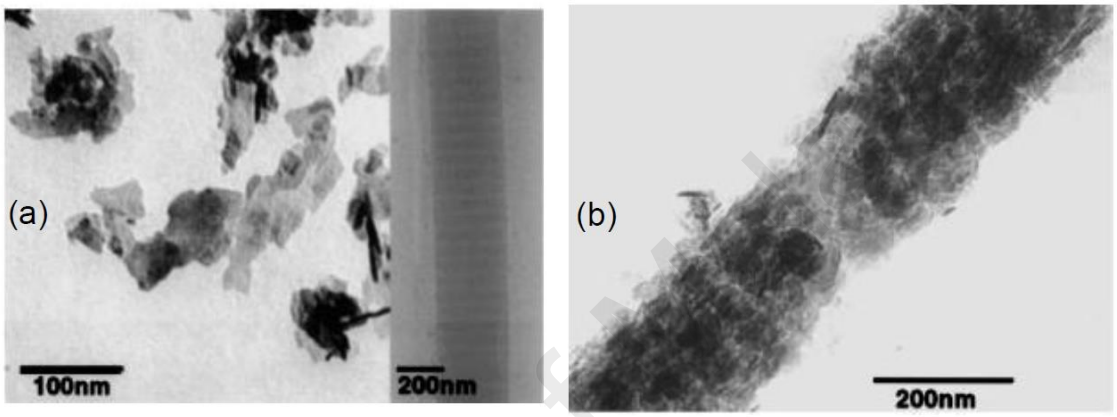

Figure 2.3: TEM micrographs of bone mineral: (a) HA nanoplates (left), demineralized collage (right); (b) mineralized collagen fiber with attached HA nanoplates (S. Weiner & H. D. Wagner, 1998)

2.1.2 Mechanical properties of bone

Bone was consider as a mineralized polymer composite in the point of view of materials science where polymer component was the collagen and HA contributed to the ceramic component. Plate shaped form of HA crystals existed in the size of tens of nanometers length and several nanometers width. The collage fibers having relatively larger size which are length of 15 μm and diameter of 40 to 70 nanometers. Both of them were aligned in such that parallel to the longer axis of the bone to give the bone exclusive anisotropy mechanically.

The calcium phosphate minerals removed by acid dissolution, a very flexible material was obtained which was the demineralized bone. On the other hand, bone which went through pyrolysis to remove collagen is very brittle. It could be summarized in such that collage contributes elasticity and toughness while HA gave the bone stiffness and hardness (S. Weiner & H. D. Wagner, 1998). In the clinical cases of hypo and hyper-mineralized bone, the amount of energy absorbable by bone before fracture was found to be decreased (Van Lierde et al., 2003). The natural bone itself was a mechanically ideal composite which is having high capacity in loading and bending without being fragile. The characteristics of high fracture and fatigue resistance is good in responding to excessive forces. In the design of composites that mimic the nature characteristics of bone, the ideal would be a substitute material that is mechanically, chemically and physically replicate the bone.

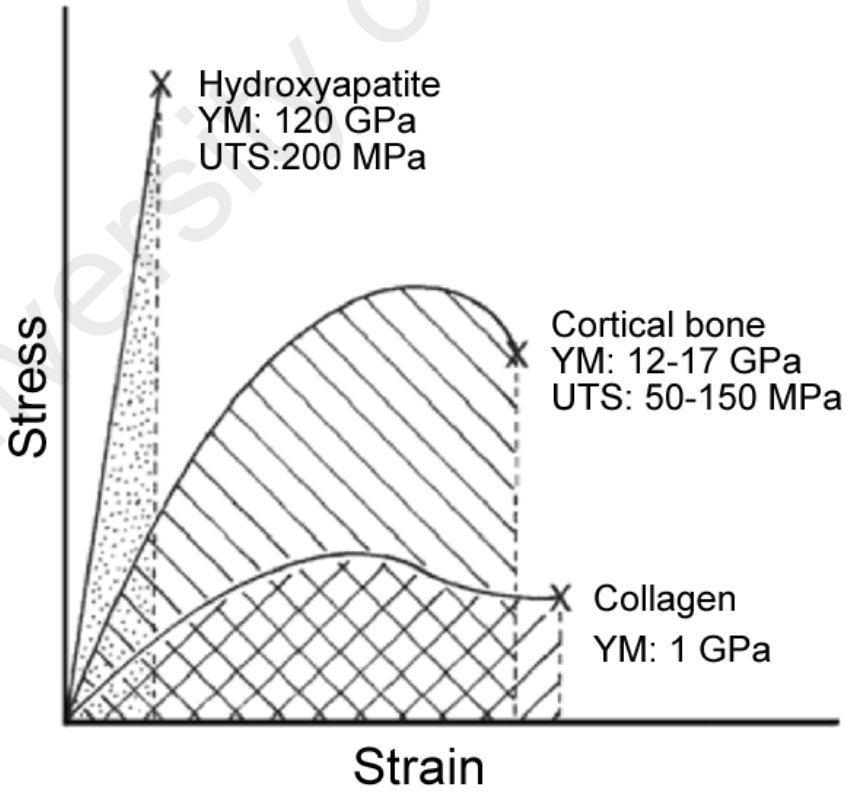

Figure 2.4: Stress – strain plot of bone and comparison of collagen, HA and bone *(Currey, Brear, & Zioupos, 1996)*

The most critical characteristics of bone to function well in supporting and protecting were stiffness and hardness. Although the protein phase was roughly 3 orders of magnitude softer than mineral, the bone was still able to hold the stiffness required even with presence of protein. The modulus of elasticity was affected by the presence of this protein phase which made it lower as compared to monolithic ceramic material even though bone contains significant percentage (60 to 70%) of ceramics phase. Various type of calcified tissues found in the human body showed distinctive different in respective organizations and mechanical properties. However all of them did share a common feature which was the protein matrix component of collagen and inorganic content of HA. Both of this 2 components were found in nano-scaled organizations which therefore able to say that bone itself was of a nanocomposite.

Natural nanocomposites from various origins such as bone and tooth were compared to study the main contributor to the superior strengths of them. Plates or needles shaped hard mineral were found in the soft protein matrix in all the samples when compared to same mineral with equivalent sized monolithic structure (Ji & Gao, 2004). One of the interesting highlight of this research was why that all the repetition of subunits found in the natural structures were all nano-sized. Assumption of the proteins existed in equivalent size to the crack in a mineral crystal that is monolithic was made. Studies concluded that there was existence of a critical point where length below, 30 nm, which the strength of fracture on a cracked crystal was similar size as that of a perfect crystal. Most of the constituents of mineral in the hard tissues did measured about the same amount.

Collagen fibers that were found to be in parallel to long axis is responding to the tensile stress as stated by the liquid crystal model. Furthermore, part of the aminoacids in the structure of collage were tilted to create distortion on their side by side arrangements. The collagen fibrils was packed with rigid HA crystals that were in contact with each other in bone that helped to prevent the tilting of intrafibril molecules and hence side to side arrangement was maintained. This exclusive structure made the bone much stiffer than those unmineralized tissues and gave them very great mechanical properties especially in compressive strength (S. Viguet-Carrin, P. Garnero, & P.D. Delmas, 2005).

2.1.3 Bone healing

Bone healing was a regenerative procedures instead of repairing the damaged section. The process was highly complicated but well controlled. Three distinctive stages that overlap in between were identified which were inflammatory, repair and remodelling stage (Ghiasi, Chen, Vaziri, Rodriguez, & Nazarian, 2017). Immediate haemorrhage could be detected after a bone fracture occurs, followed by the formation of fibrin clot (hematoma) and inflammatory response at the site of fracture due to damage of local and surrounding blood vessels. Cytokines and growth factors that induced movement of osteoprogenitor cells to the site of fracture was then released by the damaged tissues. The process of repairing initiates the removing process of blood clot, tissue and debris of cell. A fibrous collagen matrix was then laid down by the fibroblasts that residing in the deeper layer of periostum migrate while proliferate towards the site of injuries. Collagen matrix that was known as fracture callus found at both of the ends of fractured bone segments to bridge the ends. There will be formation of cartilage at the areas of the callus which is lack of blood supply and osteoblasts will starts the process of calcification. This action was triggered by the chondroblasts (Alexander C. Allori, Alexander M. Sailon, & Stephen

M. Warren, 2008). Finally, the transformation of cartilage into trabecular took place then into compact bone.

When the inflammation just started to occurs, the symptom will lasts from several days to weeks. Following inflammation was the repairing period which new vascularization takes place. The area of fracture needs to avoid any movement or else damaged could be done towards the newly formed vessels which might not be able to start process of callus calcification. In the result of that situation, only a fibrous callus will be formed which commonly known as scar. After 3 to 4 months of repairing, the area shall be able to gain original mechanical strength. During this period, it is critical to maintain the integrity of the bone implant (Xue-Nan Gu & Yu-Feng Zheng, 2010). Through the remodelling stage, the bone was able to regain the original shape and mechanical properties but it was a lengthy process which required from several months up to several years (Kalfas, 2001). A proper remodelling was highly depending on the amount of mechanical stimulus that the healing bone experiences within this period.

Throughout the process of bone healing, there were several growth factors that play important roles to function in a spatial and concentration dependent way (Patil, Sable, & Kothari, 2011). It was very important because they could regulate different phases in the repairing process. The growth factors involved are transforming growth factor-beta (TGF-β) superfamily, bone morphogenetic proteins (BMPs), insulin-like growth factor (IGF), fibroblast growth factor (FGF), platelet-derived growth factor (PDGF) and vascular endothelial growth factor (VEGF).

2.2 Hydroxyapatite

In the work of tissue engineering, hydroxyapatite was considered as one of the most efficient calcium phosphate to work on hence there was increasing demand in the usage of synthetic HA. The advantage of HA over other material was that it was able to control and lower the crystallinity. Apart from that, HA was also having great biological characteristics such as nontoxicity, lack of inflammatory and immunitary responses can be enhanced (Palazzo et al., 2007).

Due to the unique well organized way of the crystal formation of apatite in bone, there were difference between the biological and synthetic HA. The synthetic HA exhibited smaller crystal size hence having higher surface area (S. N. Danilchenko, A. V. Koropov, I .Yu. Protsenko, B. Sulkio-Cleff, & Sukhodub, 2006). This characteristics will allows the synthetic HA to adsorb more molecules (Palmer et al., 2008). Ultimately, it was critical to stimulate the biological formed HA and hence growth of HA was key to producing good material. In recent works, there are HA derived from both natural and synthetic sources as well as through various processing routes.

2.2.1 Calcium phosphates

Calcium phosphates was the top choice as material for bone substitution because of their similarity in chemical to the natural component of mineral found in bones and teeth (Viswanath & Ravishankar, 2008). Most of the calcium phosphates were marginally soluble in water but all of them would dissolve in acids. Generally by definition, all of the calcium phosphates were consist of three major elements of chemical which are calcium of oxidation state +2, phosphorus of oxidation state +5 and oxygen of oxidation state -2 (Dorozhkin, 2010). Some of the known calcium phosphates as well as their

standard abbreviation and major properties are shown in Table2.1. Generally, the calcium phosphate phase gets more acidic and soluble when the Ca/P molar ratio decreases (Wang & Nancollas, 2008).

Table 2.1: Calcium phosphate salts, name, standard abbreviation, chemical formula, Ca/P molar ratio and solubility

Name	Standard abbreviation	Chemical formula	Ca/P molar ratio	Solubility at 37°C, -log (K_{sp})
Dicalcium phosphate dehydrate	DCPD	$CaHPO_4.2H_2O$	1.00	6.73
Dicalcium phosphate anhydrous	DCPA	$CaHPO_4$	1.00	6.04
Octacalcium phosphate	OCP	$Ca_8H_2(PO_4)_6.5H_2O$	1.33	98.6
Amorphous calcium phosphate	ACP	$Ca_xH_y(PO_4)_z.nH_2O$	1.20-2.20	-
α-Tricalcium phosphate	α -TCP	α -$Ca_3(PO_4)_2$	1.50	28.5
β-Tricalcium phosphate	β -TCP	β -$Ca_3(PO_4)_2$	1.50	29.6
Hydroxyapatite	HA, Hap or OHAp	$Ca_5(PO_4)_3OH$	1.67	117.2

(Wang & Nancollas, 2008)

HA remained the most comprehensively studied bioceramic among all existing calcium phosphates due to its similarity to the natural bone (Kumta, Sfeir, Lee, Olton, & Choi, 2005). HA was not only biocompatible but also being non-toxic to the body. HA will not be detected as a harmful material by the body and also it is having characteristics of bioactive behaviour and able to integrates into living tissue which mimic the same active processes of bone remodelling. Study confirmed that HA was osteoconductive (capable to provide a scaffold or template for formation of new bone) as well as supporting osteoblast adhesion and proliferation (Dorozhkin, 2010).

2.2.2 Properties of HA

2.2.2.1 Structure

HA crystals existed in both the form of monoclinic or hexagonal unit cells. Considering from the view of thermodynamic, crystals in the form of monoclinic was less unstable and matches to stoichiometric HA (Leventouri, 2006). In the phase of monoclinic, space group $P2_1/b$, lattice parameters $a = 9.4214, b = 2a, c = 6.8814\text{Å}, \gamma = 120°$, occurance of OHs in columns on the axis of screw, pointing upward and downward in alternate, nearest-neighbour columns (Wang & Nancollas, 2008).

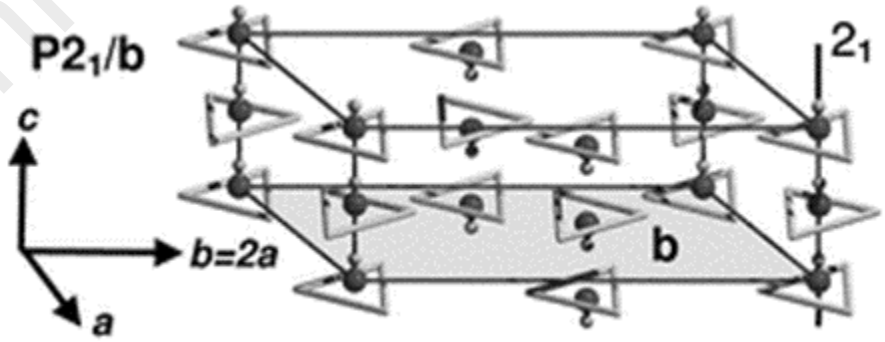

Figure 2.5: Monoclinic $P2_1/b$ HA structure (Corno, Busco, Civalleri, & Ugliengo, 2006)

HA of the form of hexagonal, space group P63/m, lattice parameters $a = 9.4176, b = a, c = 6.8814$ Å, $\beta = 120°$, generally attributed to nonstoichiometric HA (Leventouri, 2006). Most of the crystals in this form were found in biological apatites which having similar structure to the crystal in monoclinic form. However, the difference was that the columns of calcium and hydroxide groups were located in parallel channels compared to monoclinic form. These channels were ready for ion substitution to take place and this characteristic also account for the substitution in high degree that found in natural apatites (Bigi, Boanini, & Gazzano, 2016).

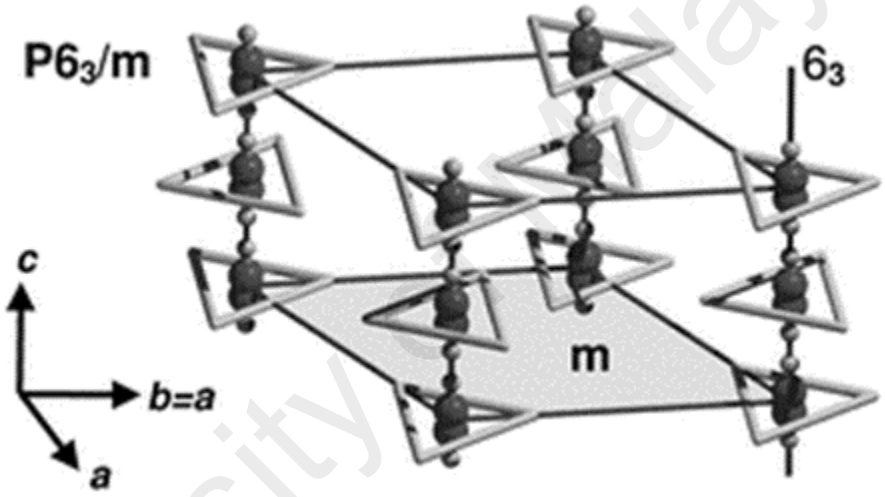

Figure 2.6: Hexagonal $P6_3/m$ HA structure (Corno et al., 2006)

2.2.2.2 Composition

HA, $Ca_5(PO_4)_3OH$, was a compound with various composition. They exist over Ca/P molar ratios from stoichiometric of 1.67 to roughly 1.5 for HA which were fully calcium deficient (Wang & Nancollas, 2008). There are also cases which the composition was found to be outside the range. In the case of biological apatites, it was found that there are multiple substitutions as well as deficiencies at all ionic sites. Among all the compounds, it was important to highlight B-type carbonate HA which has carbonate

substitution. In this compound, phosphate ions were substituted by carbonate (Leventouri, 2006).

2.2.2.3 Phase stability

With the assist of a typical solubility phase diagram where solubility isotherms were expressed as plots of log [Ca] as function of pH, the stability of calcium phosphate (CaP) phases when in contact with aqueous solutions can be understood. Any salt whose isotherm lies below another for a given pH value was found to be relatively more stable and also less soluble (Fernandez et al., 1999). The most stable compound that found under the condition of pH 4.2 to 12 at 37℃, body temperature, was the HA. The study found that HA was least soluble down to pH 4.2 at this temperature.

However, there were also other important factors in determining the likelihood of the formation of preferred phases of crystal in a solution that was supersaturated with several different phases which was kinetic factors (Koutsopoulos, 2002). Phase formation of HA was found to be slower than of either OCP or DCPD. Even though the thermodynamic driving force of HA was much smaller, observation of a larger portion of the kinetically favoured phase was found during simultaneous phase formation. It was very important for the discussion of the likelihood of formation of precursor during calcium phosphate precipitation which was affected by the balance between kinetic and thermodynamic factors.

2.3 Hydroxyapatite derived from natural source

There were a handful of researcher working on the development of HA from natural sources. Currently developed natural source including bovine bone, fish bone, porcine bone, eggshells, coral and seashells. Although there were many tested natural sources, bovine bone was the most well established sources due to the ease of obtaining samples as well as complying halal requirement. Characteristics of natural HA were highly depending on the method of extraction applied (Younesi et al., 2011). Commonly in natural HA, there existed of carbonate ions as impurity as opposed to the synthetic HA. The carbonated ions found in natural HA appears to be an excellent material for bioresorbable bone substitutes (Suchanek et al., 2002). The critical advantage of extracting HA from natural sources offers was that no usage of harmful chemicals is involved in the process (Silva, Bertan, & Moreira, 2005).

2.3.1 Bovine bone

When bovine bone undergoes heat treatment, nanocrystalline apatite was observed when the calcination temperature used was from 700℃ to 1000℃ (Ooi, Hamdi, & Ramesh, 2007). However, HA phase was found to be decomposing into minor phase of β-TCP when the temperature goes beyond 1000℃. As the temperature increased towards 1200℃, the minor phases also increased. This was confirmed by the intensity of XRD characteristic peaks data. After carried out heat treatment at various temperature, 750℃ was found to be the best temperature as the XRD patterns (Figure 2.7) showing well-defined and sharp peaks of pure HA phase (Niakan et al., 2014).

When the bovine bone was heat treated at 850℃ for 5-6 hours, data from XRD spectrum showed that HA in the phase of hexagonal was obtained (Yoganang, Selvarajan,

Wu, & Xue). The heat treated sample was crush into powder for observation under scanning electron microscope (SEM). Images showed that the powder was in highly irregular shapes. However, an undesired disease-causing agent was not observed on the heat treated samples (Ozyegin, Oktar, Goller, Kayali, & Yazici, 2004).

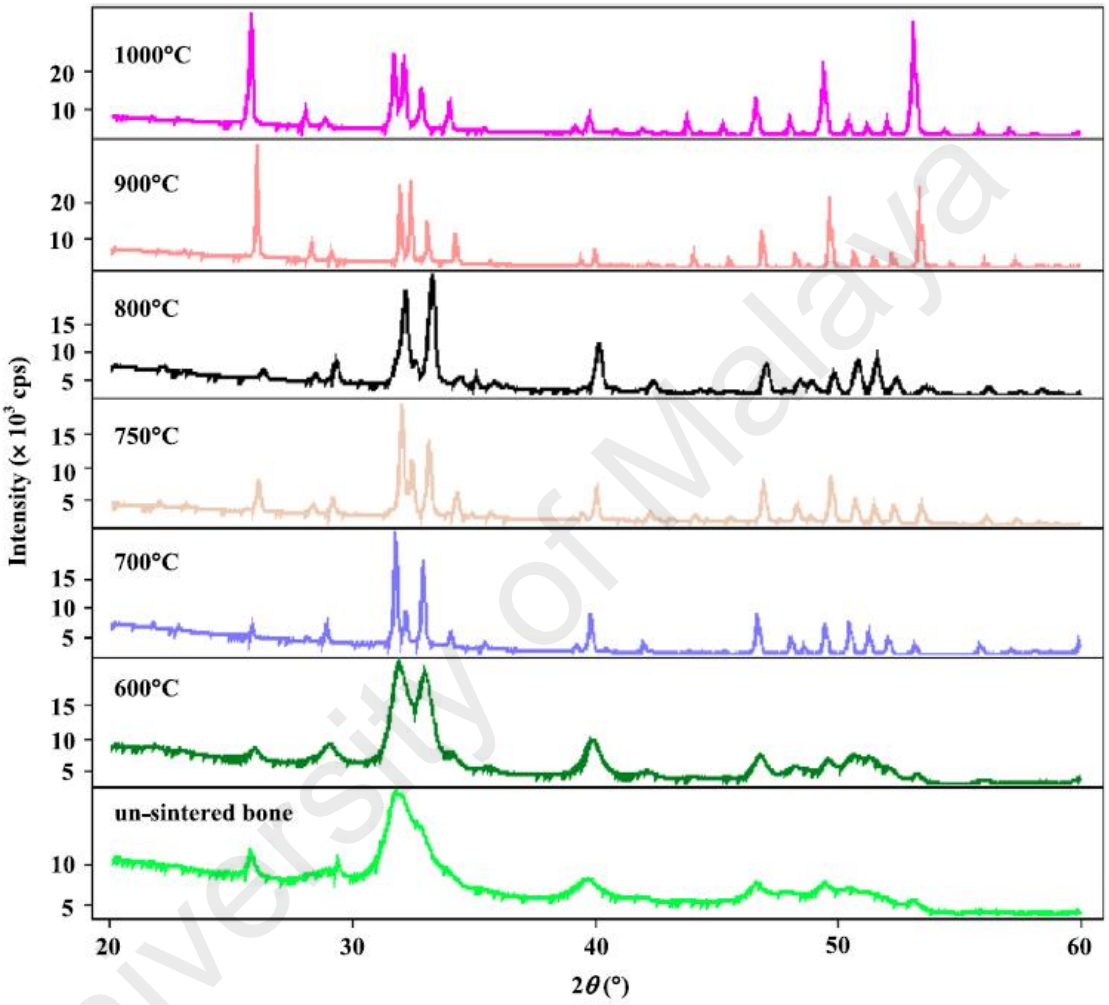

Figure 2.7: XRD signatures of raw bovine bone and heat treated bone samples as varying temperature. All peaks belong to the HA phase. It was identified that 750℃ was the optimum temperature. (Niakan et al., 2014)

In the observation of microstructure of bovine bone based HA, no change in the orientation of HA crystallites was observed (Benmarouane, Hansen, & Lodini, 2004). The

samples was heat treated at 625℃ for 3 days. It was then analysed by neutron diffraction pattern which showed that all the HA crystallites still directed along the axis of the bone.

Development of high purity HA nanopowder from bovine bone via vibro-milling technique was studied. Dried bone was heat treated at 800℃ for 3 hours and then grounded by vibro-milling at several times. Analysis of XRD patterns show that pure HA phase was found in all of the grounded powders of bone. After vibro-milling for 2 hours, SEM images revealed that nanoneedle-like shape of HA powders with diameter less than 100nm were found (Ruksudjarit, Pengpat, Rujijanagul, & Tunkasiri, 2008).

Using bone ash as a starting material, researcher synthesized HA and TCP to study the characteristics of blended composition (Lorprayoon, 1989). At first, bone was calcined at 700℃ for 8 hours. Obtained bone ash exhibit nano-scaled particles when observed under transmission electron microscopy (TEM). The calcined bone ash was then dissolved and performed precipitation at various pH value. Heated for 2 to 3 hours at temperature ranging from 1230 to 1280℃, two phases was found in different range of pH. When the pH was at 8.0-8.5, TCP was obtained while pure HA phase was observed at pH of 9.7-10. At the pH value of 7 which was neutral, the reaction medium was inactive hence calcium deficient HA was obtained due to slow reaction of Ca^{2+} and PO_4^{3-} ions. When the pH was increased, the mobility of ions increased and lead to higher rate of reaction. The pH value of 9 was determined as best for synthesis of HA nano-particles to produce compound with Ca/P molar ratio 1.67 (Palanivelu, Saral, & Kumar, 2014).

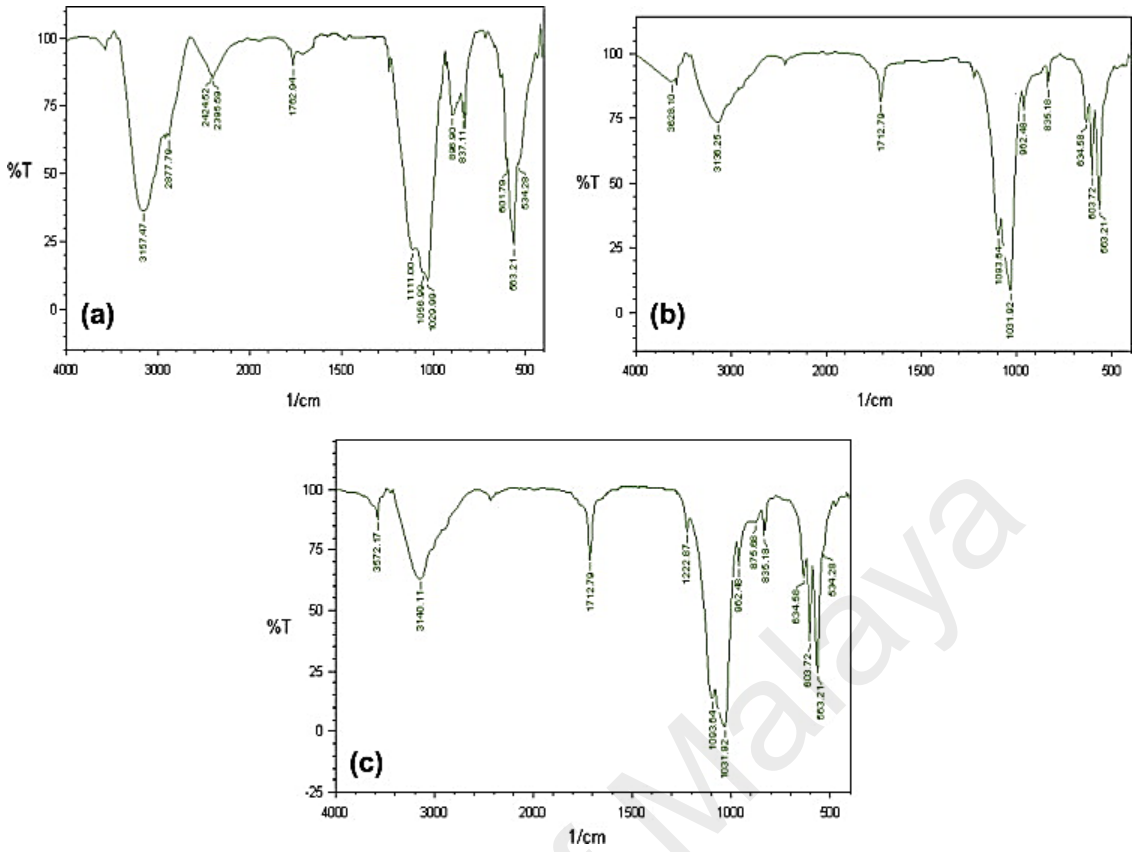

Figure 2.8: FTIR spectrum of synthesized HA at various pH values (a) pH 7, (b) pH 9, (c) pH 11 (Palanivelu et al., 2014)

2.3.2 Fish bone

Utilizing the waste from fishing activities, study was done on developing biological HA from fish bones. Not only that it could help on reducing the waste but also adding value to the cheap source of by-products. Bone of tuna and sword fish was chosen for heat treatment. At 600℃, it was found that the powder was phase pure HA but when the temperature increased to 950℃, biphasic material was found. The powder obtained was a mix of HA and β-TCP in the ratio of 87:13. In vitro studies confirmed that all the powders obtained were non-cytotoxic (Boutinguiza et al., 2012).

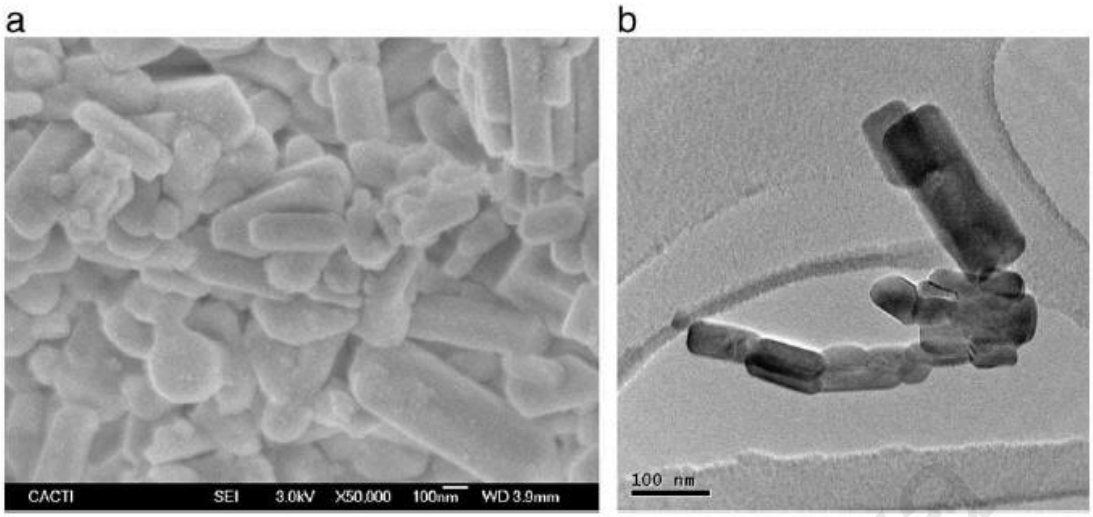

Figure 2.9: (a) FESEM and (b) TEM micrographs of the poweders from heat treated fish bones at 600℃ (Boutinguiza et al., 2012)

One of the key highlight of HA was the ion-exchange properties which was useful sorbent of heavy metals and radionuclides (Galambos, Suchanek, & Rosskopfova, 2012). However the capacity of ion-exchange was highly influenced by the composition and crystallinity of HA. Focusing on the effects of major trace elements, a study based on the calcined bone of tuna, yellow tail, greater amberjack and horse mackerel was established. The temperature chosen was 400℃, 600℃, 800℃ and 1000℃ while HA was formed starting from 600℃. When calcined above 800℃, tuna bone which having high Ca/P ratio showing decomposition of highly crystalline HA into CaO phase. However in the case of horse mackerel which having high magnesium content show HA of less crystalline and higher amount of β-TCP formed. It was suggested that phase pure HA of high crystalline could be obtained by heat treating fish bones with high Ca/P molar ratio and low in magnesium content (Goto & Sasaki, 2014).

Table 2.2: Elemental composition (calcium, phosphorus, sodium, potassium and magnesium) found in fish bones calcined at 600℃ for 2 hours. Traces of strontium, zinc, manganese and silicon were all below 0.01mmol g^{-1}

Notation	Elements (mmol g^{-1})					Molar ratio	
	Ca	P	Na	K	Mg	Ca/P	(Ca+Mg+0.5Na+0.5K)/P
Yellow tail	9.42	6.15	0.71	0.06	0.13	1.53	1.61
Greater amberjack	9.33	6.19	0.66	0.10	0.15	1.51	1.59
Tuna	9.41	6.06	0.67	0.04	0.13	1.55	1.63
Horse mackarel	9.03	6.34	0.59	0.11	0.21	1.42	1.51

(Goto & Sasaki, 2014)

2.3.3 Porcine bone

Characteristics of porcine bone derived HA at elevated temperatures was done and 700℃ was determined as the temperature that the bone started to decompose (Haberko et al., 2006). In result of the calcination, calcium oxide and carbonate groups were partially removed from the sample. Simultaneously, growth of crystalline became intensive while the specific surface area decreased. The powder also noticed to be shrinking.

Naturally, bones contain water and this will lost during heat treatment and hence reducing the weight of the samples. It was found that the raw bone sludge underwent thermal decomposition of four stages. The first stage is endothermic when the temperature

was increased up to ~200℃, desorption of water from the surface of sample took place. By observing the thermo gravimetric analysis (TGA) curve (Figure 1.10), the sample lost 3.11% of weight at this stage. Stage 2 and 3 overlapped and both corresponds to the decomposition of organic compounds. This 2 stages happened within the temperature range of ~200℃ to ~600℃. The earlier stage contributed by burning of protein which reflects weight loss amounting to 13.12% while the later stage was contributed by burning of fat. Upon hitting ~800℃, the sample underwent last stage of weight lost which corresponded to the dehydroxylation processes. Hydroxyapatite compounds were decomposed thermally while carbonate groups were eliminated (Sobczak-Kupiec & Wzorek, 2012).

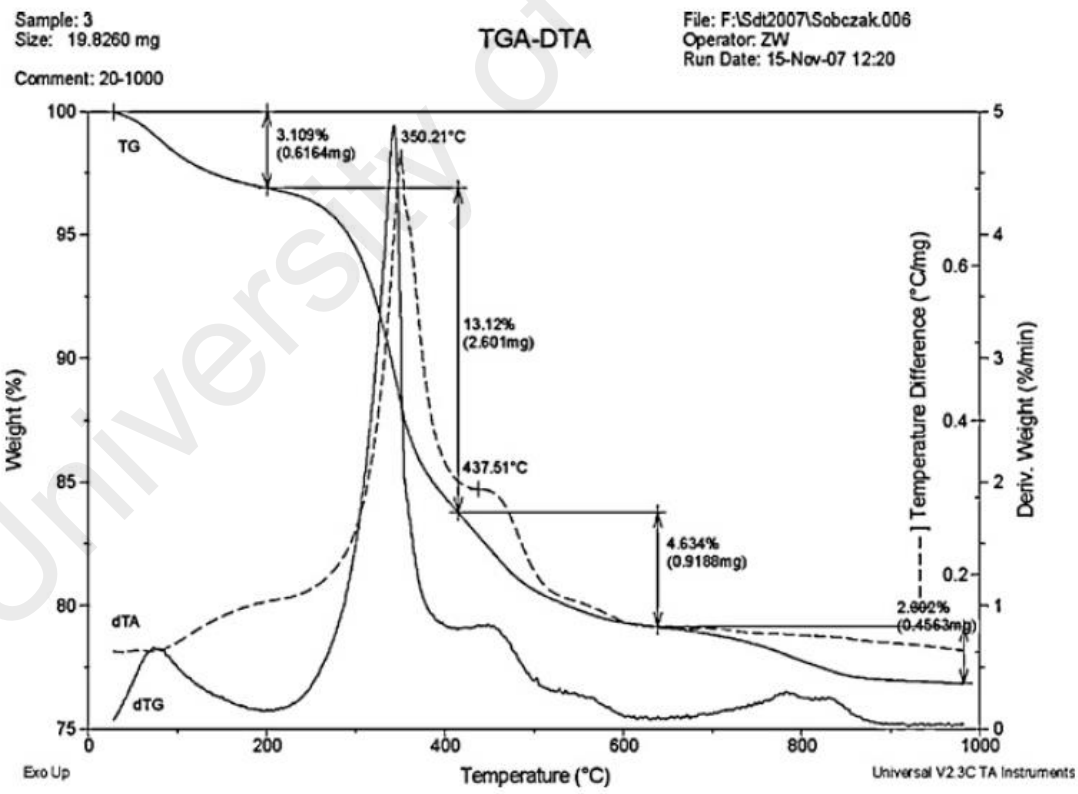

Figure 2.10: TGA curve of calcination of porcine bone (Sobczak-Kupiec & Wzorek, 2012)

2.3.4 Eggshell

Eggshell could be utilised as a source of developing natural HA as well. The difference of preparing HA from bone and eggshell is that HA could be obtained by direct heat treatment of bone while eggshell required synthetically derived precursors step. Sintering of eggshell-derived HA in atmospheric pressure over the temperature range of 800℃ to 1400℃ was studied. The calcined as calcium precursor prepared via the wet chemical precipitation method was found to be phase pure HA. Upon sintering, the samples remained pure HA phase up to temperature of 1250℃ but decomposition into α-TCP and TTCP was observed in the range of 1300℃ to 1350℃. Further sintering at 1400℃ resulted in melted sample (Kamalanathan et al., 2014).

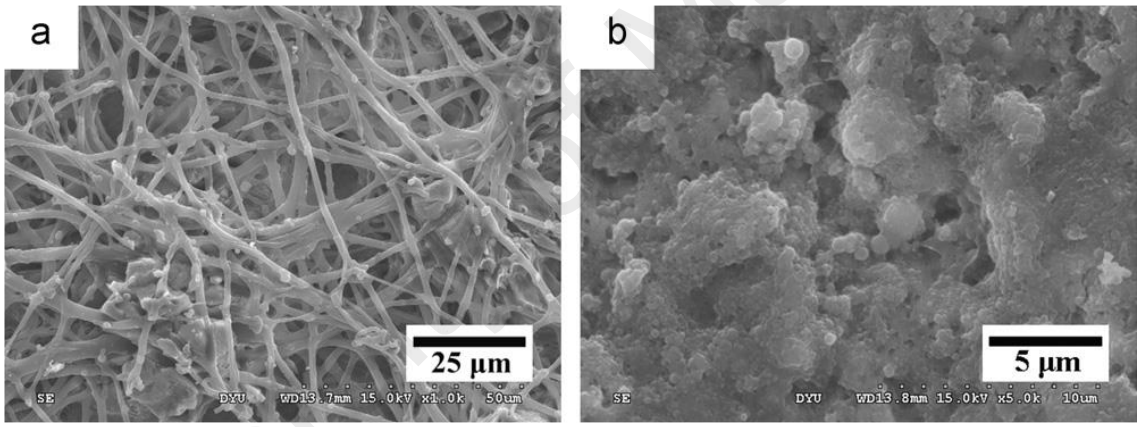

Figure 2.11: SEM images of (a) inner surface and (b) outer surface of eggshell (Ho, Hsu, Hsu, Hung, & Wu, 2013)

The motivation behind choosing eggshells as source of deriving HA was such that the eggshell was treated as garbage of food processing, baking and hatching industries. Not only by varying the synthesis method, researchers also tried to employ several biomolecules from fruit waste into the hydrothermal synthesis of eggshell-derived HA. The fruit waste extract studied were grape, sweet potato and pomelo peels which contains various biomolecules such as polyphenolic compounds, beta-carotene (Negro, Tommasi,

& Miceli, 2003), carotenoids (Al-Weshahy & Venket Rao, 2009) and essential oils (Senevirathne, Jeon, Ha, & Kim, 2009). Through various analysis, it was found that the involvement of biomolecules influenced shape formation of crystal, crystal size and crystal morphology (Wu et al., 2013). Eggshell-derived HA with the influence of pomelo peelings exhibited good aspect ratios and also mimic the crystalline structure of HA in natural human bone.

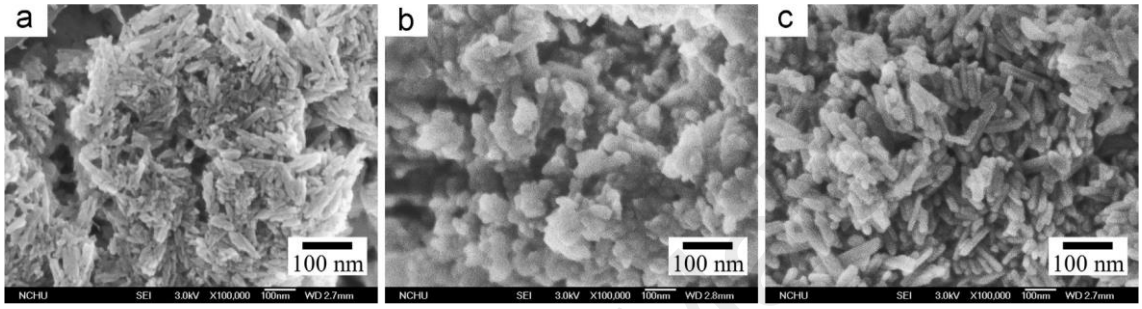

Figure 2.12: SEM images of hydrothermal synthesized HA using three kinds of biomolecular templates in waste at 150℃ for 74 hours. (a) Grape peel, (b) sweet potato peel and (c) pomelo peel (Wu et al., 2013)

2.4 Sintering of hydroxyapatite

HA powder that calciniced will be sintered to a temperature before melting yet high enough to allow the diffusion of solid-state and to permit bonding of the particles. Normally this is done in an atmospheric environment but controlled temperature. The main purpose of carrying out calcination is to combust air content and also removal of compounds that are thermal labile which may affect the good bonding of sintered sample (ASM International, 1991). Sintering stage which involve higher temperature triggered the sample to undergo solid-state diffusion and bonding of the particles in the powder. The sample will then be allowed to cool to room temperature in a controlled environment to prevent oxidation if the sample was directly exposed to air and also experienced thermal shock.

It was very important to control the sintering parameters as they directly affect the outcome of HA powders (Rao & Kannan, 2002). HA with high density was desired as it could prevent contamination of human fluid into the interfacial area between coating of HA and the Ti-alloys in hip joint replacements. In oppose, replacement of fractured bone requires porous HA to allow ingrowth of the natural and artificial bone to occur which would create strong bond (Juang & Hon, 1996). HA powder that was sintered at 1000℃ for 1 hours showed high density and the sample has almost pore-free morphology (Sung, Lee, & Yang, 2004).

Sintered HA was determined to be having very good density value which was 99.9% of the theoretical value of HA due to fine particles were produced during the sintering stage. The HA powder which consist of very fine particles having the advantage of high surface area which favours the solid-state sintering. At the same time, the amount of surface energy decreases is in proportional to the decreases of free energy during sintering process (Sung et al., 2004). In other words, the sintering behaviour of HA powder could be controlled by varying the particle size of powder. Improvement in crystallinity of sintered HA was observed when HA powders with specific surface area of 68m^2/g sintered for 1200℃ for hours (Kim, Kong, Lee, & Kim, 2002).

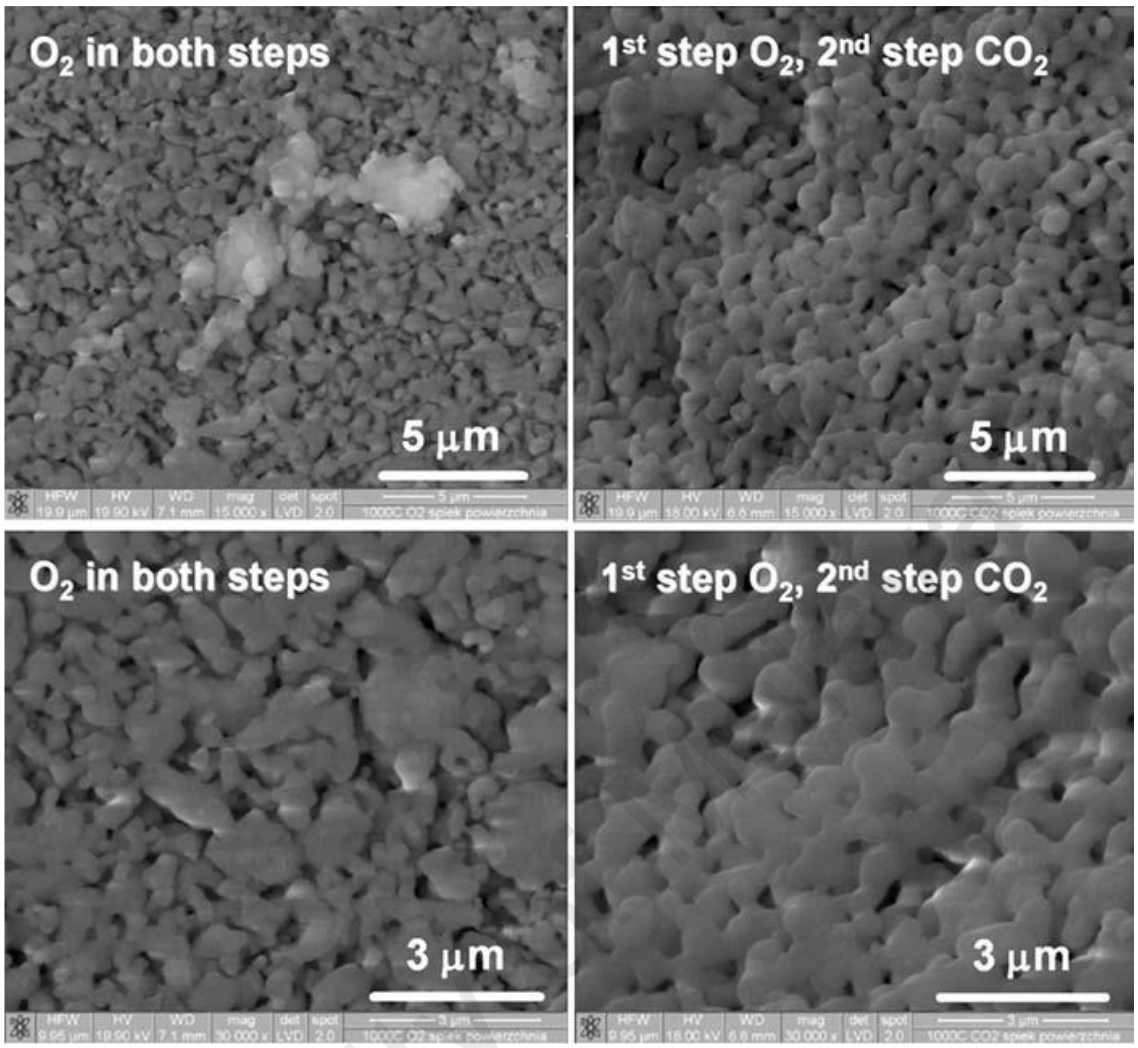

Figure 2.13: SEM micrographs of HA powder sintered in atmosphere of oxygen or oxygen and carbon dioxide at 1000℃. (Janus, Faryna, Haberko, Rakowska, & Panz, 2008)

To eliminate agglomerates in the powder of HA, it was tested that the powder could be ball milled after calcination at 900℃ for 4 hours. Other studies also supported that by employing various sintering treatments the average particle size and distribution could be increased (Juang & Hon, 1996). To study the sintering behaviours, dilatometry and density measurement was used. Dominating the properties of sintered sample was found to be fluidity of HA powders as well as driving force. Sample with about 55MPa of bending strength and fine grain size was obtained when sintering process was done at 1250℃. SEM analyses supported that this idea that grain size increased exponentially

with the increase in sintering temperature (Ramesh, 2001). The HA phase was stable when sintering temperature used was below 1400℃ for 2 hours but decomposition into TCP, TTCP and CaO was observed when the temperature was higher. The contributing factor to the prevention of dehydration of OH- groups from the HA matrix was assumed to be by the high humidity of content present in sintering atmosphere slowing down decomposition rates.

2.5 Summary

Throughout various researches done, it was safe to say that HA derived from natural bone was very safe to use in biological application due to no chemical was involved in the calcination processes. Apart from that, the great biocompatibility characteristics also made HA derived from natural bone a very good candidate material to be used as bone implants to replace or repair fractured hard bone. Natural bone would only require direct heat treatment in oppose that other natural sources such as eggshell, coral or seashells would require further synthesis be it chemically or with the help of biomolecules. Bovine was the best choice among all and calcination at temperature ranging from 600℃ to 1000℃ also showed phase pure HA while 750℃ determined to be the optimum temperature. Sintering of bovine bone-derived HA powder also showed promising sample when the temperature used was below 1200 ℃ without the HA decomposing into secondary phases.

CHAPTER 3: METHODOLOGY

3.1 Introduction

In the early stage of the research, journal papers and books were reviewed for useful information especially raw materials and processing methods used. After summarizing the collected highlights, potential raw materials and processing method could be chosen. Study will be focusing on the raw materials that is yet to be well established which in this case are caprine and galline bone.

Since that there are lack of study done, this research work is aimed to study the potential of hydroxyapatite derived from the animal bones to be used in biomedical applications with bovine bone as reference group. The experiment was carried out in lab with well-planned procedures and schedules to make sure progress on time. All collected data will be analysed before being accepted to be in the final documentary. Group with rejected results will be repeated to minimize any possible error. Analysis of data will be carried out to make sure that they are able to fulfil the objective of this study.

Detailed discussion on the results will be carried out before making conclusion to this research work. This research project will be completed with submission of the project report. Timeline of this research project is presented in Figure 3.1 to make sure that the progress adhere to the initial plan.

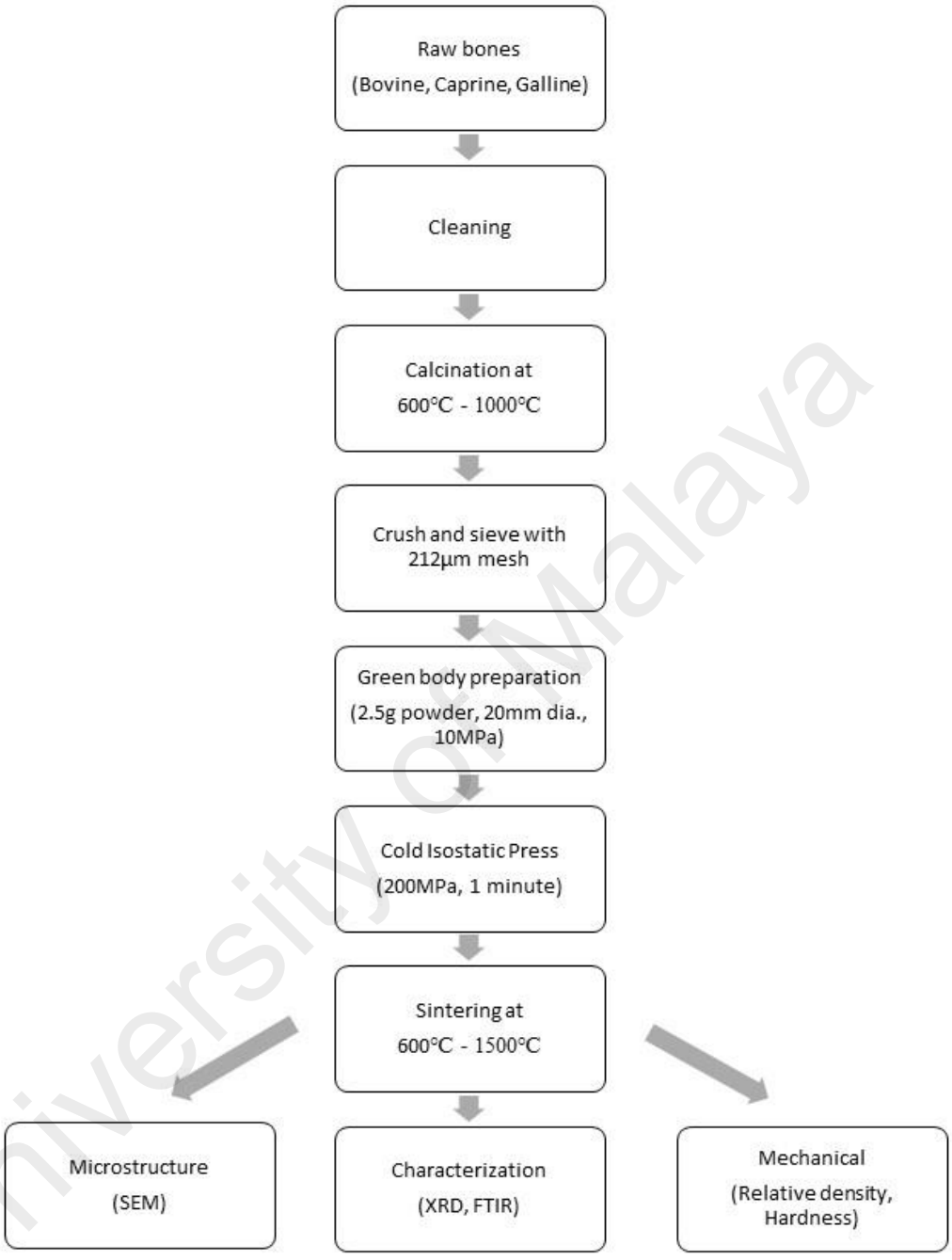

Figure 3.1: Flow chart of the research project

3.2 Specimen preparation

3.2.1 Powder preparation

Raw femur bones of bovine, caprine and galline were collected from local stall as food waste. The received bones were thoroughly washed and cleaned to remove any flesh and fat residues attached on the bone. The bone marrows were also cleaned to make sure the bones were as clean as possible. Autoclave process was done to ensure all the external protein attached were fully removed. It was done at 100°C for 1 hour by using a gas pressurized cooker. After the bones were cooled, they were rinsed with tap water and then soaked in acetone for 1 hour to clean residual grease. Lastly, the bones were dried in box oven at 70°C for 3 hours.

The dried bones were broke into smaller pieces and calcined in an electric furnace (LT Furnace, Malaysia) at temperature ranging from 600°C to 1000°C. Temperature ramp rate was fixed at 10°C per minute with holding time of 2 hours. They were then crushed with pastel and mortar into fine pieces followed by sieving with 212 μm metal sieve to ensure uniform particles.

3.2.2 Bulk specimen preparation

Bulk specimens in disc shape were formed by compacting the calcined bone powders in mold of 20mm cylindrical opening at 10 MPa using a hydraulic bench press (C106C, Power Team). Each formed disc weighing 2.5g. After each forming, the dies were cleaned using a penetrating oil and water displacing spray (9.3 oz aerosol can, WD-40 Company) to avoid contamination. The disc samples were then Cold Isostatically Pressed (KJYu, Shaxi Golden Kaiyuan Co. Ltd) at 200 MPa for 1 minute. To prevent the samples from stacking or mixing, each of the samples were placed separately inside each

finger of a powder-free latex glove. The thumb of each glove was left empty to provide space for expansion in case of any excess air trapped upon pressurizing. All the openings of the gloves were tied and sealed tight before being compacted.

Sintering was done in atmospheric condition using an electric furnace. Sintering temperature ranging from 600°C to 1500°C. Ramp rates were 10°C per minute for both heating and cooling. The hold time set was 2 hours for each sintering process.

3.2.3 SEM sample preparation

All the sintered specimens were wet grinded and polished to acquire flat and smooth surface on one face. This smooth surface will be used for carrying out SEM observation, and microhardness test. This processes were carried out on a semi-automated grinding machine. The wet grinding process started with commercially available SiC sand paper of 1000, 1500, 2000 and 2400 grit to flatten the surface. Following that, the surface was then polished with 1μm diamond paste (Mecaprex diamond compounds, Presi) to obtain a surface which is optical reflective.

Samples that were sintered above 1300°C were also thermally etched at 50°C below sintering temperature. The ramp rate was also 10°C per minute but only held for 30 minutes. This process help to reveal the grain boundaries for easier observation.

3.3 Characterization

3.3.1 XRD

X-ray powder diffraction (XRD) is a technique of analysis that could be done rapidly to identify phase present in a crystalline material. This method is based on the theory discovered in 1912 by Max von Laue. It is found that the wavelengths of X-ray

are similar to the spacing of planes in a crystal lattice when crystalline substances acting as a three-dimensional gratings for diffraction. The simple idea is detectors receiving the diffracted rays that directed at the sample by an X-ray tube.

All the calcined bone powders were characterized with XRD (PANalytical X'Pert^3, Netherland) to analyse the phase presents. The analysis was carried out using Cu-Kα as the source of radiation at scan speed of 0.5° per minute and a 0.02° step of scan. Crystalline phase compositions of samples were matched to the standard reference JCPDS card no. 01-074-0565 for hydroxyapatite (HA) and 00-09-0169 for β-tricalcium phosphate (β-TCP) in the system. Through analysis of the XRD peak pattern, optimum calcination temperatures were identified.

3.3.2 FTIR

Fourier transforms infrared spectroscopy (FTIR) belongs to a method of infrared spectroscopy analysis. Infrared radiation was directed through the sample. Some amount of radiation will be transmitted through while some will be absorbed by the sample. The detector will detects and generate a graph to show the spectrum that been absorbed or transmitted creating a unique molecular profile. The uses of FTIR included to identify unknown substances, to determine quality of a sample and to determine the percentage of components in a compound.

To identify the composition of samples upon heat treatment, FTIR analysis (NICOLET 6700) was performed. This step can ensure that all the bone powders calcined at chosen optimum temperature were free from organic compounds leaving only pure

inorganic apatite compounds. This is very important due to that the traces of organic compounds could be source of allergens or causing immune response which will be very complicated to treat and lethal in most cases.

3.3.3 SEM

Scanning electron microscope (SEM) is a microscope that utilises electrons instead of light source for the formation of image. The discovery of this technique in early 1950's greatly assisted in the development of new interest areas of research especially for the field of medical science. The high resolution of SEM opened up the possibility for researchers to study in larger variety of specimens that were not possible to be done on traditional light microscope.

In this study, SEM (Phenom ProX, Netherlands) was used to observe the morphology of both raw bones and sintered specimens. This would allow the comparison between structure of sintered specimens to the raw natural bones. Grains and pores were observed with the captured micrographs.

Heyn linear intercept method was adopted to measure the average grain size of the sintered samples, following ASTM standard E112-96 (ASTM, 2004). 5 known test lines were randomly drawn on the print of SEM micrographs to calculate the average grain size. The counting including number of intercepts between the test line and grain boundaries. If the end point of a drawn line touches exactly a grain boundary, it will be taken as half intersection. A full intersection will be scored for tangential intersection with grain boundary while 1.5 will be scored for intersection that falls on meeting point

of 3 grains. An equation proposed by Mendelson was used to calculate the average grain size (Mendelson, 1969).

$$Average\ grain\ size = 1.56 \times \frac{Total\ length\ of\ the\ test\ line}{Number\ of\ intercepts}$$

3.4 Relative density

Archimedes' principle was adopted to evaluate the relative density and apparent porosity of sintered specimens. Following ISO18754 standard, distilled water was used as the immersion medium. This method is also known as the hydrostatic weighing where the measurement is considered to be easier and more accurately without measuring the volume. The specimen is first weighed in air, then weighed immersed in water and lastly in air after immersion. The relative density is then calculated with the formula:

$$Relative\ density = \frac{W_a}{(W_c - W_b) \times \rho_{HA}} \times \rho_w \times 100$$

Where,

W_a = weight in air

W_b = weight immersion

W_c = weight after immersion

ρ_{HA} = density of HA, 3.16 g/cm^3

ρ_w = density of distilled water at 25°C, 0.99997 g/cm^3

3.5 Microhardness

Microhardness test is also known as microindentation hardness testing. It is used to measuring the hardness of a given materials at microscopic scale when macroscale test is not usable. The test force used is less than 1 kilogram for this test. An impression was made by using a precision diamond indenter and then the length of indention was measured by the aid of microscope.

Sintered samples that are polished were tested for microhardness (H_V) using Vickers hardness tester (Shimadzu, Japan). The test parameters used were load of 25g with holding time of 5 seconds for making indentation. For better accurancy of the hardness values, measurements were taken at three different locations on the samples and then averaged. The hardness value in MPa is calculated by multiplying HV by 9.807.

3.6 Summary

As a summary to this chapter, the HA samples were prepared from calcined raw animal bones that were crushed and sieved. Conventional sintering technique was used to sinter the formed green bodies. Microstructure of the sintered specimens were observed using SEM while XRD was used for characterization. On top of that, the relative density of the sintered specimens were calculated using water displacement method. Lastly, mechanical properties of the specimens were studied using microhardness.

CHAPTER 4: RESULTS AND DISCUSSIONS

4.1 Introduction

In this chapter, various results obtained from the experiment are presented with interpretation and analysis of the results.

4.2 XRD

The phases present in the sintered specimens could be determined both qualitative and quantitatively through XRD patterns. Generally, it could be observed that all 3 different bones produced different peak patterns. All the XRD patterns obtained were compared with standard card JCPDS card no: 01-074-0565 for stoichiometric HA, 00-09-0169 for β-TCP and 00-029-0359 for α-TCP. All 3 raw bones showed low crystallinity of the HA phase and the pattern span across broad range. With the increase in sintering temperature, higher intensity of peaks reflected the increased in crystallinity phase of HA. Highly crystalline phase of HA would produce sharp and narrow peaks.

Generally, the lower temperature specimens showing increasing crystallinity in phase pure HA but started to transform into β-TCP when the decomposition temperature is reach, which is 1350°C for bovine, 1250°C for caprine and 800°C for galline. When the temperature goes further upward, peaks corresponding to α-TCP were observed. The observation of mixture of peaks corresponding to HA and TCP is also known as biphasic for the higher temperature specimens.

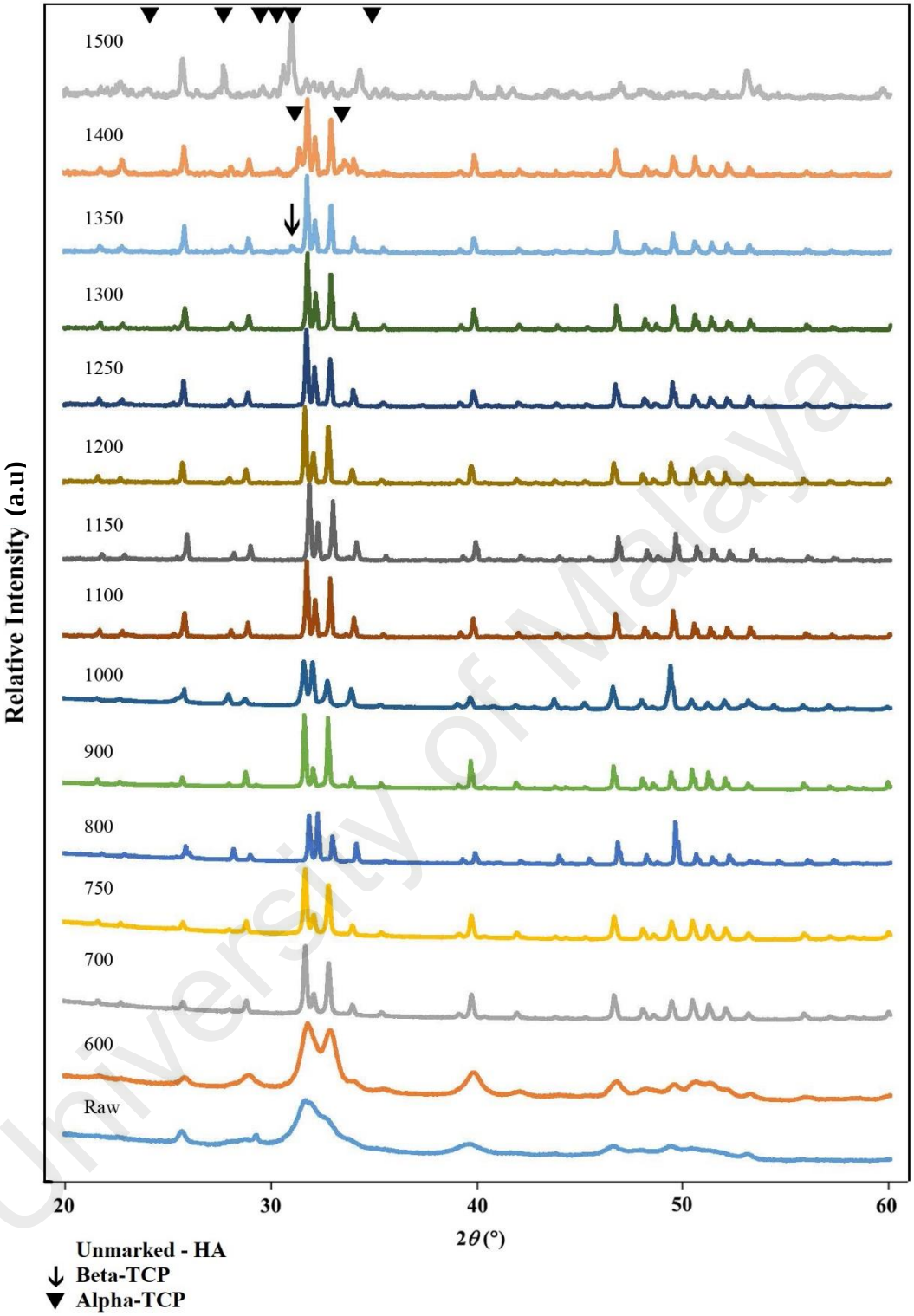

Figure 4.1: XRD for bovine bone sintered at various temperature, arrow showing β-TCP peak, triangle showing α-TCP peaks while unmarked peaks correspond to HA

The specimens from bovine bone stay phase pure up to 1300°C. At 1350°C, small peak corresponding to β-TCP was observed while peaks corresponding to α-TCP were observed when the temperature were further increased to 1400 ° C and 1500. It is observable that on 1500°C, the highest peak corresponds to α-TCP instead of HA as of other temperature range.

The increasing in sharpness and relative intensity of peaks show that through sintering, the specimen gained high crystalline phase of HA. By comparison, the raw bone and specimen sintered at 600°C broad and low peaks. One noticeable point of this study is that the sintered specimens did not show phase change on lower sintering temperature which observed by other study (Jinlong, Zhenxi, & Dazong, 2001).

In this study, the sintered specimens of caprine bone stayed phase pure up to 1200°C which is slightly lower than the specimens of bovine bone. The phase change occurred earlier but only β-TCP was observed up to 1500°C. As compared to specimens of bovine bone, more peaks corresponding to β-TCP were observed here which suggest that percentages of β-TCP phase were increasing.

The XRD patterns obtained from sintered specimens of galline bone shows similar trend as that of bovine bone which phase change to β-TCP and then α-TCP occurred. Among the 3 bones sources, galline bone was the earliest to have phase changing. It was observed that the peak corresponding to β-TCP started to show at 800°C. β-TCP peaks were observable continuously up till 1100 ° C. From 1150 ° C to 1500 ° C, peaks corresponding to α-TCP were observed.

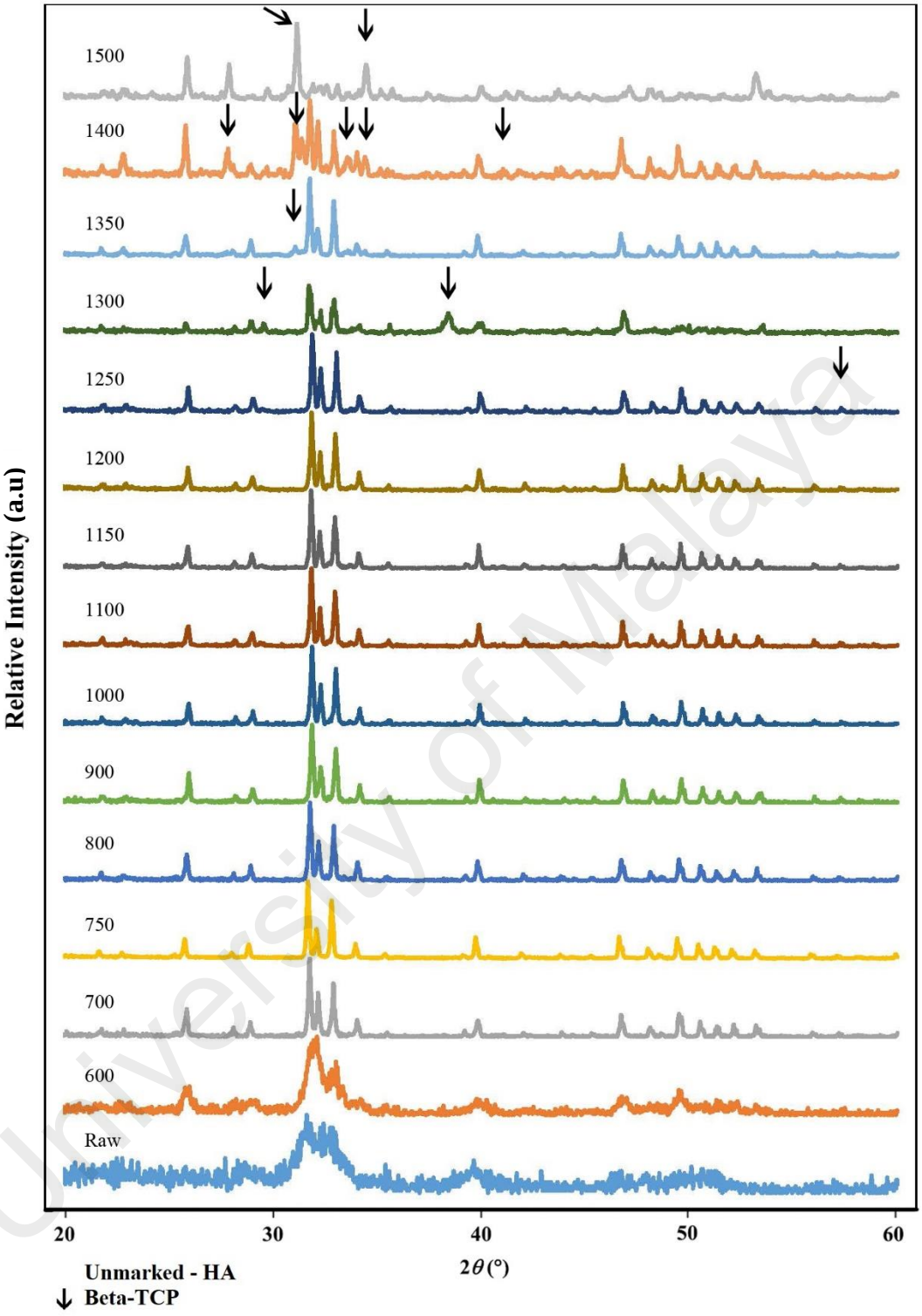

Figure 4.2: XRD for caprine bone sintered at various temperature, arrow marked correspond β-TCP peak while unmarked peaks correspond to HA

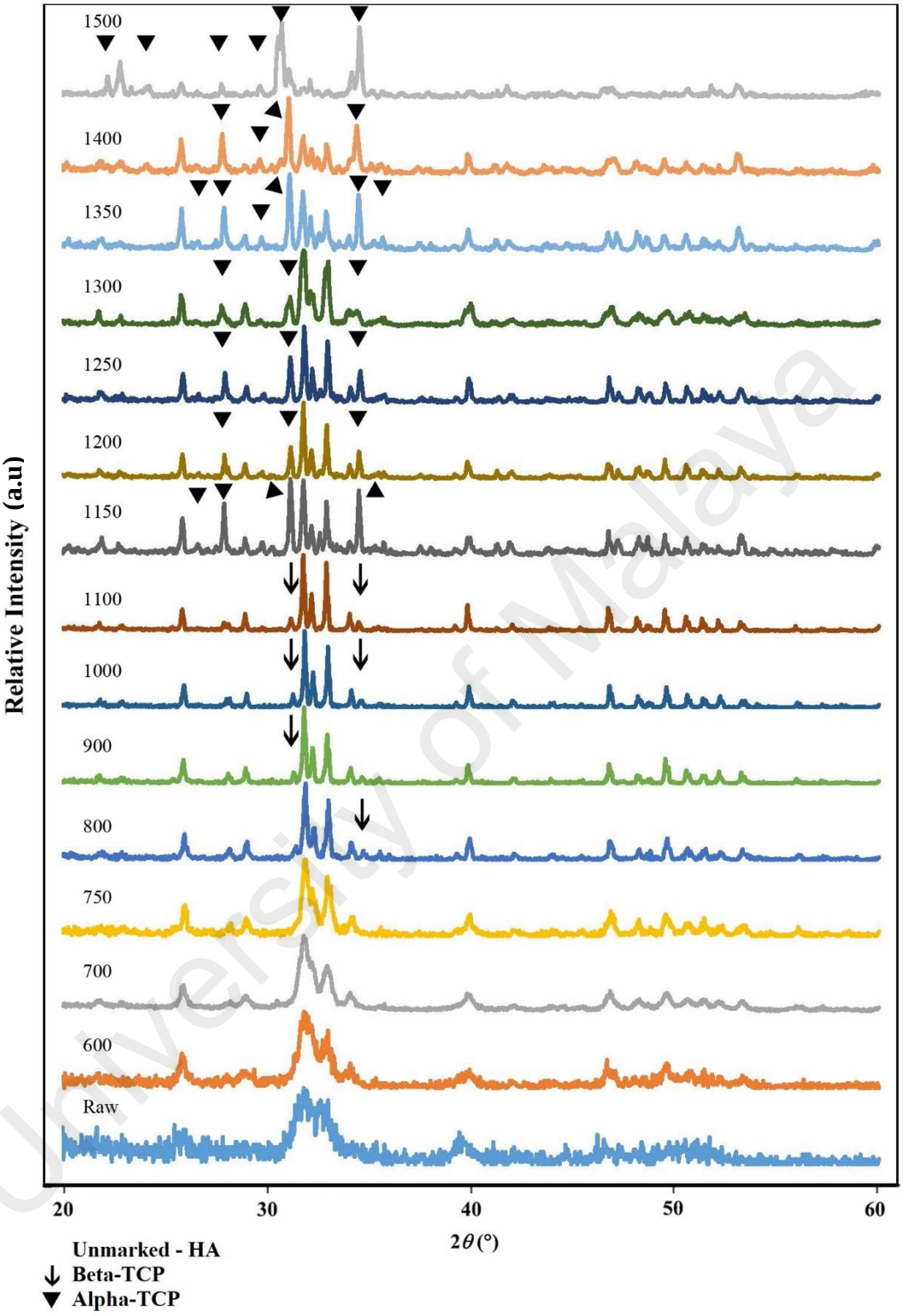

Figure 4.3: XRD for galline bone sintered at various temperature, arrows showing β-TCP peak, triangle showing α-TCP peak while unmarked peaks correspond to HA

Although phase change occurred, the main peaks were corresponded to HA phase up to 1300°C. Sintering beyond that temperature, the highest peaks were corresponded to α-TCP phase. Not only that specimens of galline bone had phase change occurred at lower temperature, the percentage of TCP phase were also higher as compared to bovine and caprine bone.

The specimens of galline bone sintered at lower temperature does show phase pure HA but the peaks were not as well defined which suggesting that the crystallinity of HA phase were lower. The decomposition in galline specimens occurred earlier mainly due to the difference in characteristics of bone. Bovine and caprine bones are denser and having more particles of bone while galline bone are having higher amount of total protein which easily burnt off during the heat treatment process. The amount of total protein found in per mg of dry bone for all 3 bone sources were reported to be bovine 79.7µg, caprine 120.1µg and galline 128.8µg (Aerssens, Boonen, Lowet, & Dequeker, 1998).

4.3 FTIR

Optimum temperature was determined for all three type of bones which was 750°C. When heat treated at least at this temperature, all three type of bones produce phase pure HA and well defined peaks which shows high crystallinity. To confirm the calcined bones were free from any organic compounds which would meant not fit for use in biomedical application, FTIR study was done. When analysing the spectrums, only absorption peaks corresponding to HA should be found on these calcined samples.

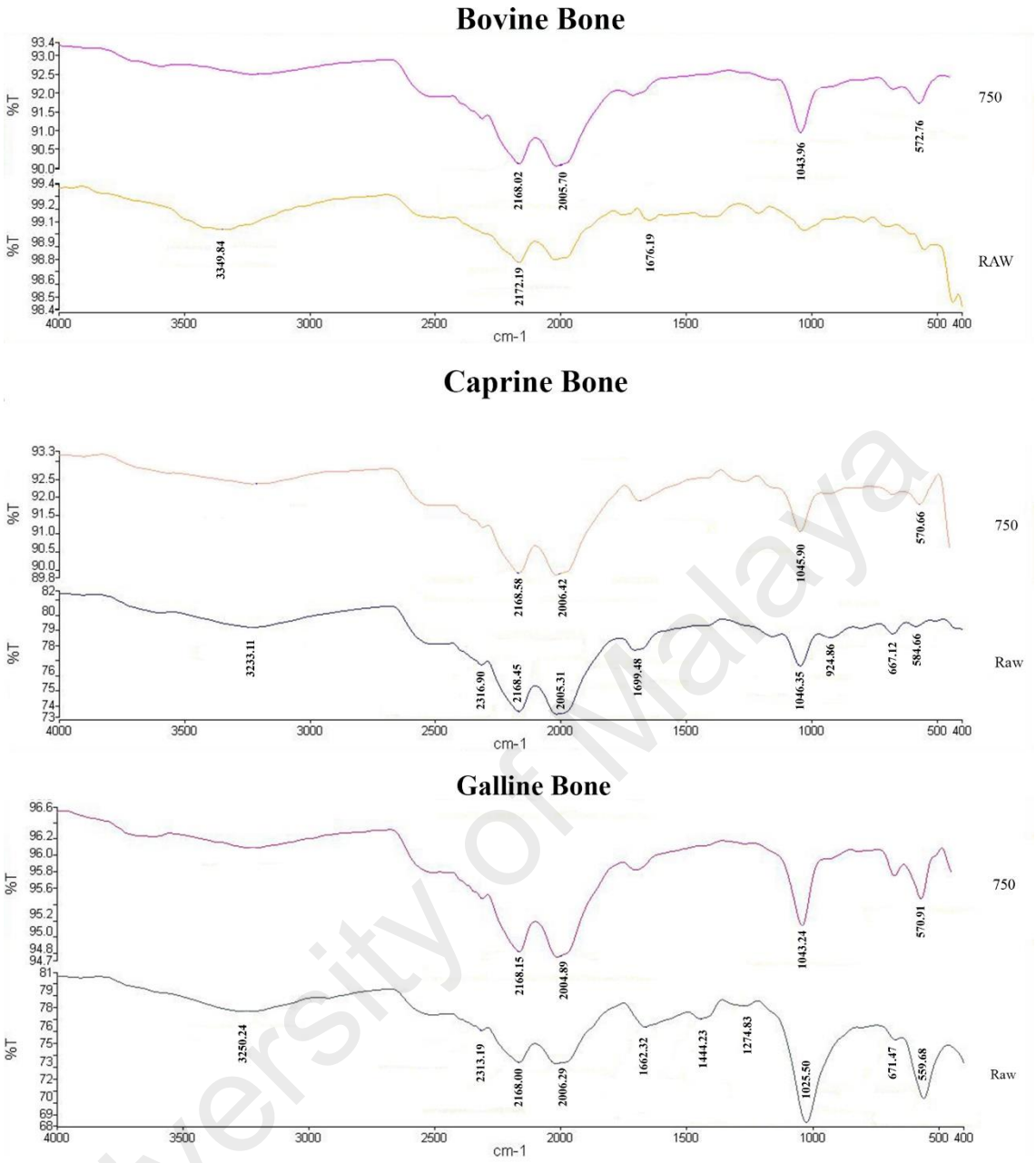

Figure 4.4: FTIR spectrum of raw and calcined bone samples

Finding from the FTIR analysis having good agreement with the results observed from XRD. The calcined samples showing only HA absorption peaks. Comparing the FTIR spectrum of raw bones also confirmed that they are in good agreement with previous study showing that the increasing amount of total protein per mg of dry bone

from bovine, caprine and galline bones (Aerssens et al., 1998). The higher percentage of absorption translating to higher concentration of the compounds.

All three raw bones do have common bands which corresponded to the organic compounds of O-H and C=O. They occurred in the range of 3300-2500 cm^{-1} and 1820-1660 cm^{-1}. Upon calcination, all of these were completely removed. On top of the above compounds, sample of raw caprine and galline bones also showing extra absorption peaks. The peaks on 2316.90 cm^{-1} of caprine bone and 2313.19 cm^{-1} of galline bone also corresponded to O-H bonds. Raw galline bone sample had 2 additional absorption peaks which are not found on other bones, they respectively corresponded to aromatic compound on 1444.23 cm^{-1} and alkyl bromide on 671.47 cm^{-1}.

It can be said that all the calcined bone samples were free from any organic compounds and exist in pure HA form. This can be observed from the absorption peaks around 1036.2 cm^{-1} and 567.4 cm^{-1} which they corresponded to PO_4^{3-} ion. It was observed that all calcined samples showed maximum absorption occurred around 1036.2 cm^{-1} that corresponded to PO_4^{3-} ion which is in good agreement with reported data (Ooi et al., 2007). Absorption peak with low intensity around the region of 1950-2200 cm were corresponding to the overtones and combinations of the PO_4^{3-} in v_3 and v_1 modes (Walters, Leung, Blumenthal, LeGeros, & Konsker, 1990).

4.4 SEM

There are two major part that can be identified on the natural bones, which are the densed cortical part and porous trabecular part. All the raw bones used in this study were taken from the cortical part of femur bone. Although the part of bone chosen was the

densed part but there were also holes on the surface of the raw bones. The structure of the raw bone is such so that the cell could attached easier and growth along the bone.

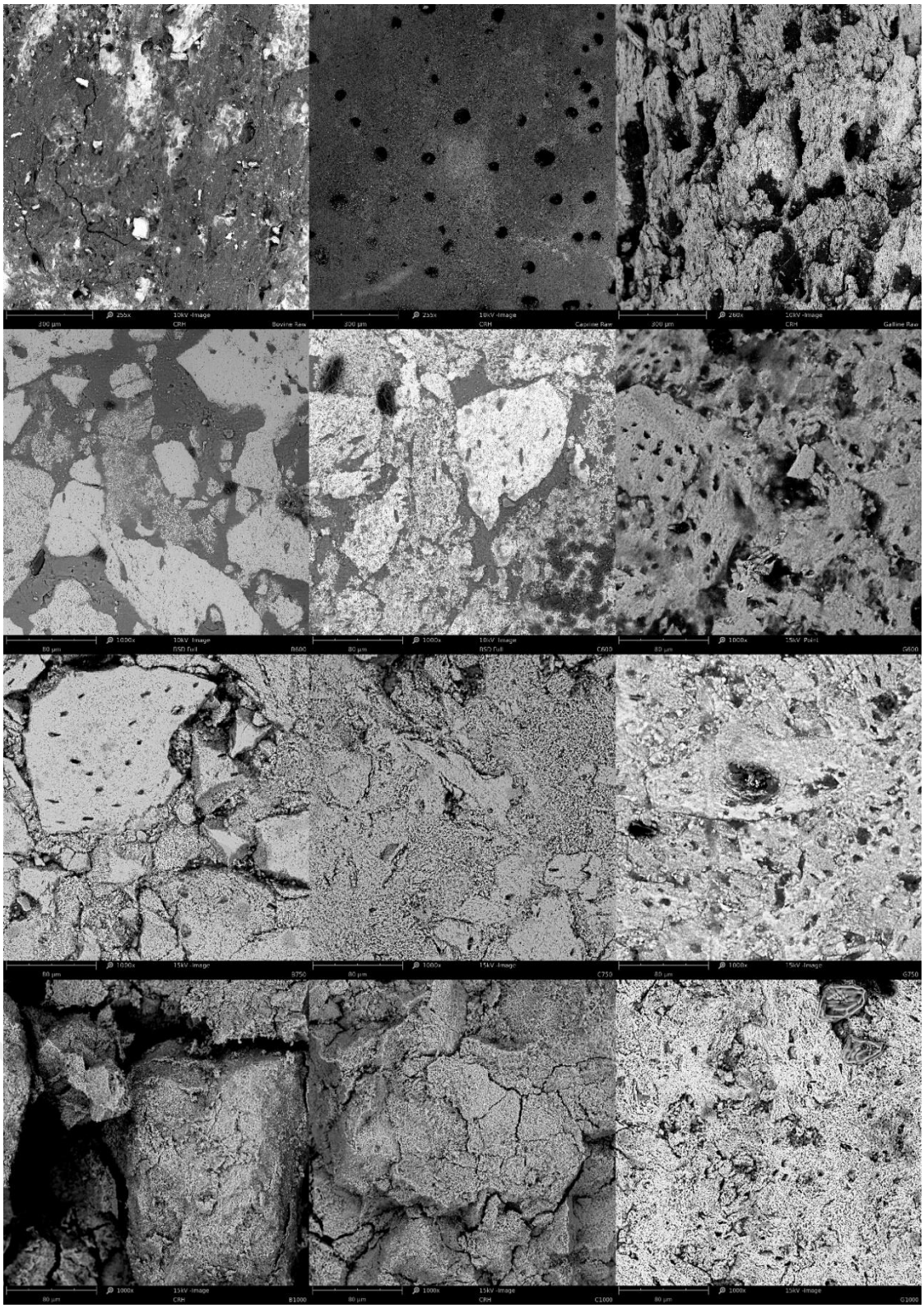

Figure 4.5: SEM micrographs of sample from bovine, caprine and galline bones (left to right) at raw, 600°C, 750°C and 1000°C (top to bottom)

SEM micrographs of raw and sintered samples were shown in Fig 4.5. It could be observed that the samples sintered at 600°C appears to be very similar to the raw bones, especially sample of galline bone. When the sintering temperature were increased to 750°C, it is observable that the samples got denser. At this stage, both samples of bovine and caprine shown the start of formation of fibrous network structure which was not observed on the galline. Further increasing the sintering temperature to 1000°C, the fibrous network structure were clearly visible on all samples. The porous network structure is very suitable for application in orthopaedic because it promotes tissues to be attached onto and proliferation of cells (Sopyan & Kaur, 2009).

The sintered samples shown fibrous network structure up to the sintering temperature of 1300°C. Although the samples did get reduction in porosity but there were no good formation of grains that will give the sintered sample better mechanical properties. Upon close inspection as shown in Fig 4.6, it was observed that there were well defined shape of crystal formed and also signs of grain growth.

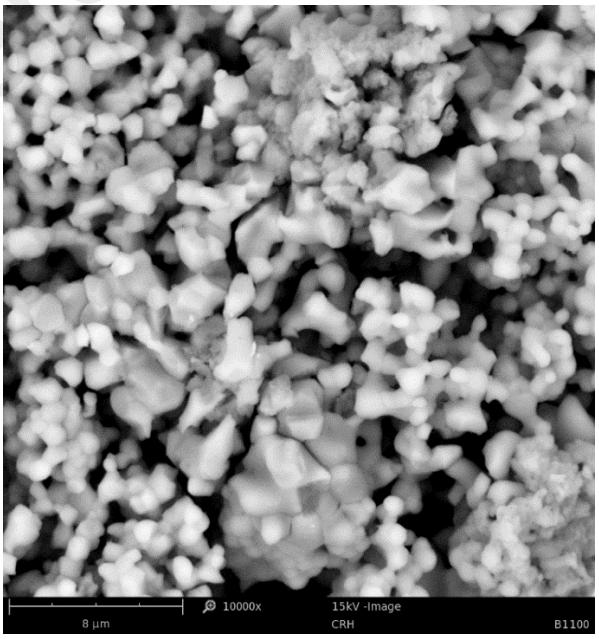

Figure 4.6: 1100°C sintered sample of bovine at 10000x magnification

4.5 Grain size

The average grain sizes of bovine, caprine and galline bones specimens sintered at 1350°C, 1400°C and 1500°C were presented in Fig 4.7. The grain size for specimens sintered at lower temperature was unable to be measured due to the absence of clear grain boundary formed on the specimens. Overall, the grain size of sintered bone specimens increased with the increase in sintering temperature.

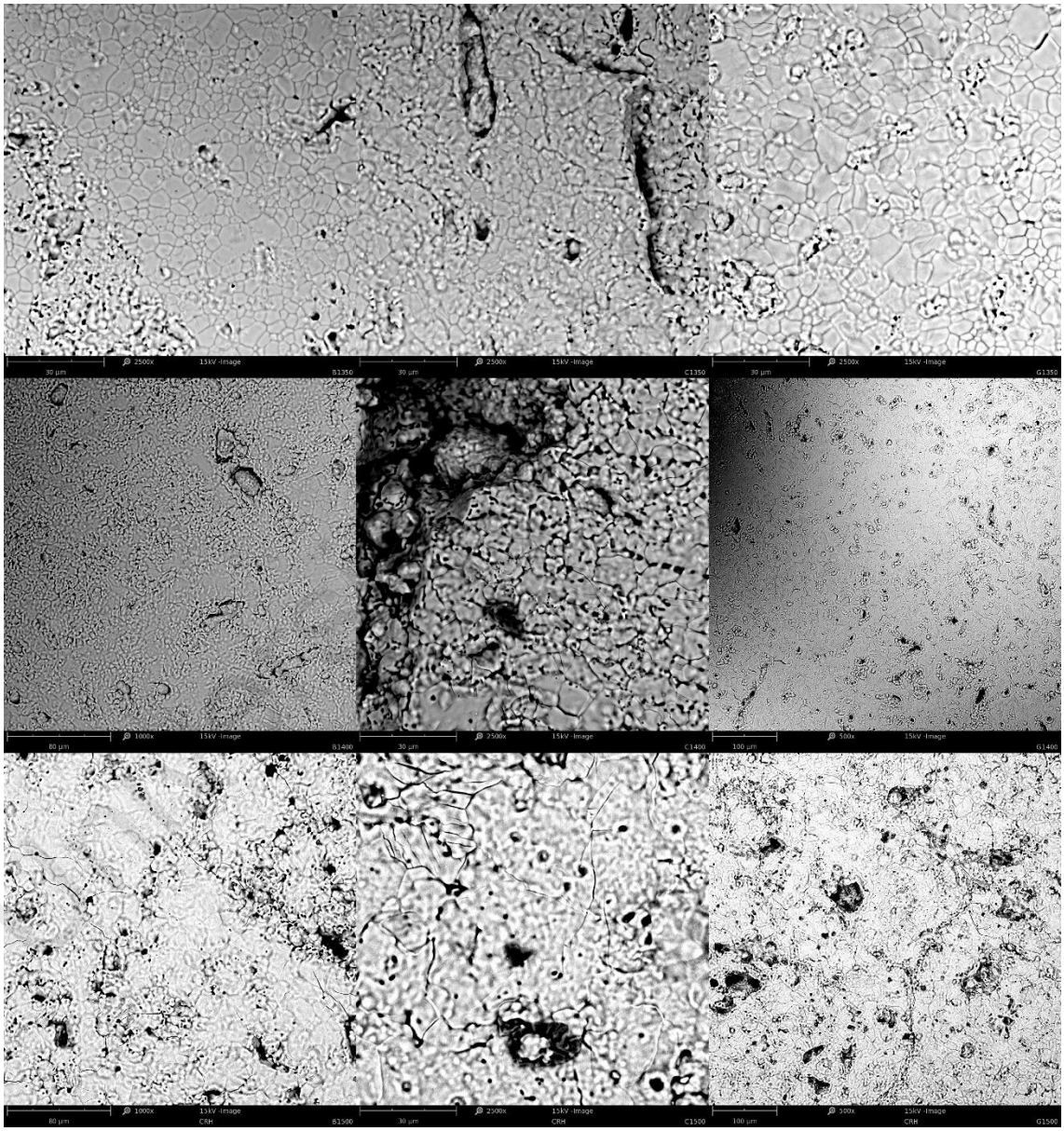

Figure 4.7: SEM micrographs of sample from bovine, caprine and galline bones (left to right) at raw, 1350°C, 1400°C and 1500°C (top to bottom)

When sintered at 1350°C, all 3 bone specimens showed about the same average grain size which were 5.366 µm, 5.675 µm and 7.155 µm respectively. Going further to 1400°C, all 3 type of bone specimens increased in average grain size but the specimens of bovine and caprine bone remained closely while galline bone specimens gained significantly. The respective average grain size for three of the sintered bone specimens were 9.354 µm, 10.12 µm and 18.97 µm. The average grain size of bovine and caprine bone specimens doubled as before while the galline bone specimens almost tripled.

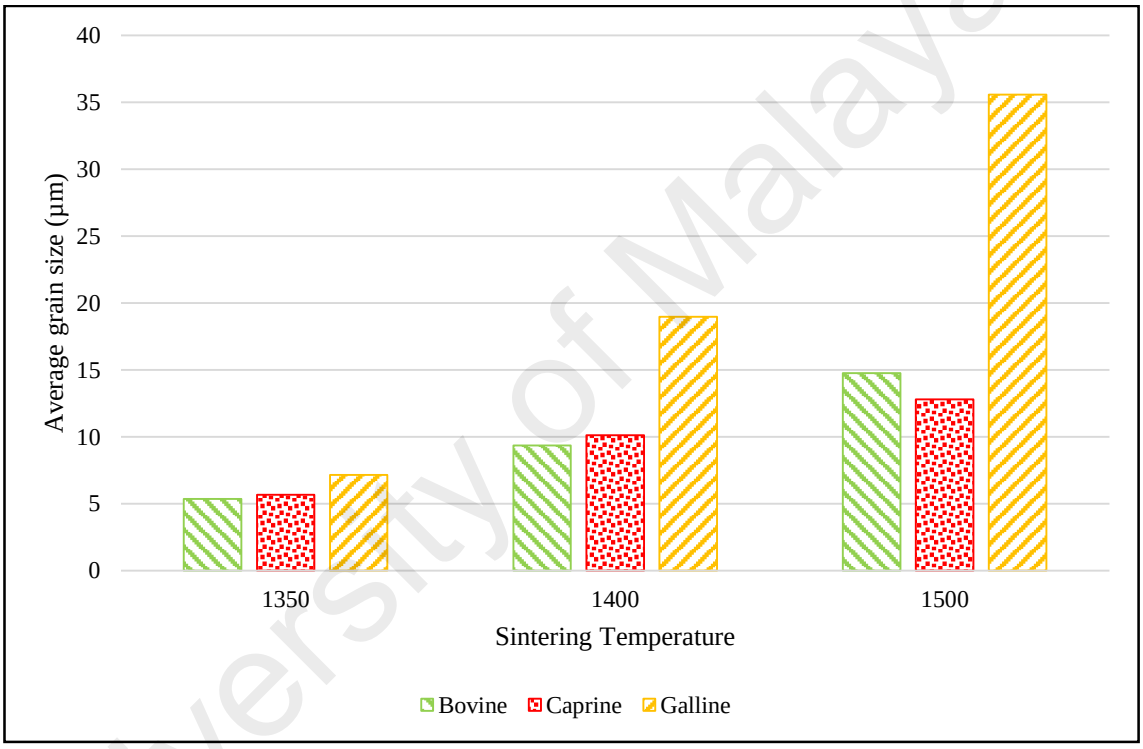

Figure 4.8: Graph of average grain size against sintering temperature

Further comparing with average grain size of specimens sintered at 1500°C, it was clear that the galline bone specimens rapidly growth in grain size which contributed to the higher relative density and also hardness. Sintered at this temperature, the average grain size of bovine, caprine and galline bone specimens were found to be 14.76 µm, 12.8 µm and 35.57 µm respectively. The specimen of sintered caprine bone showing lower rate of grain size growth at this moment.

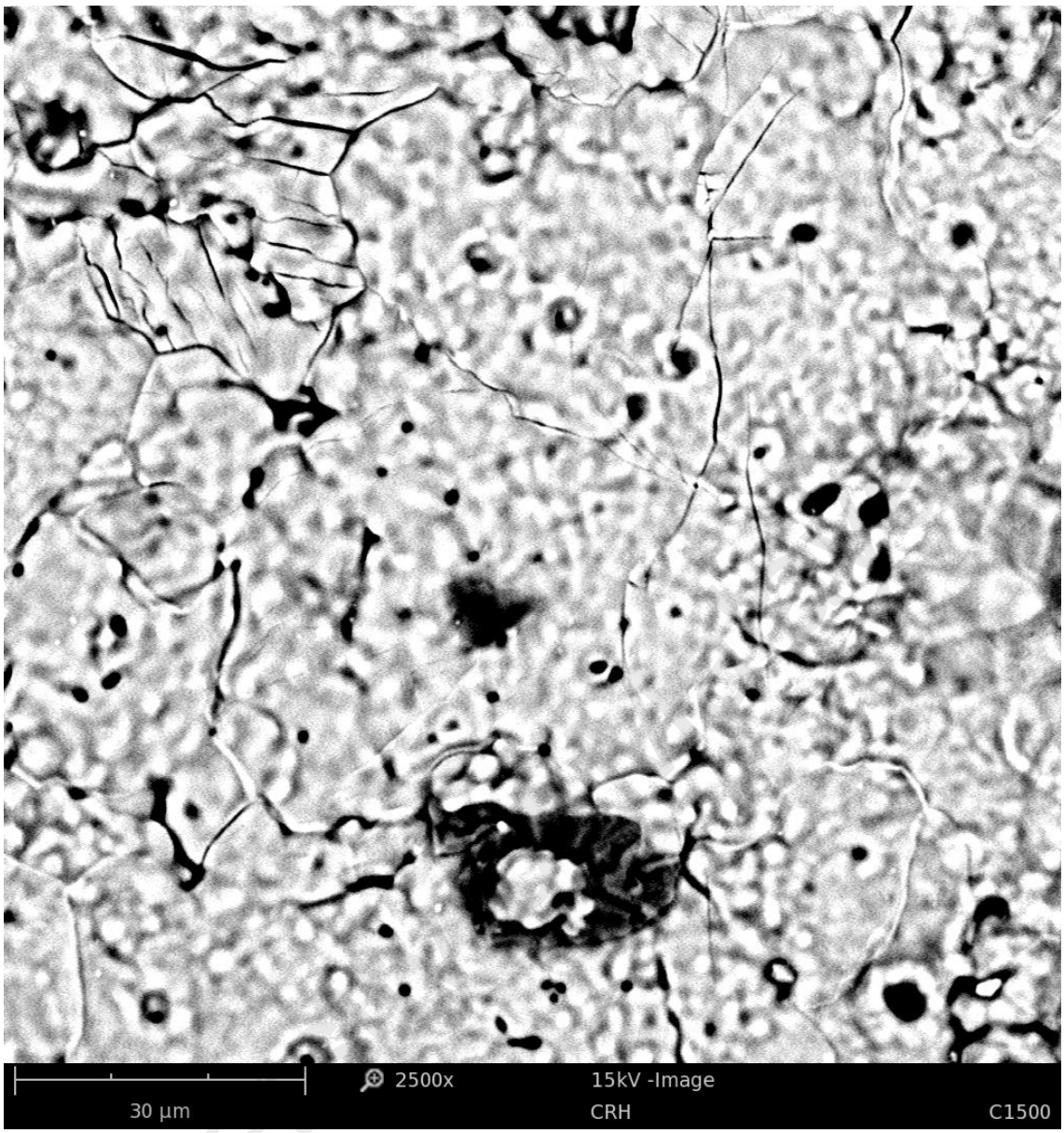

Figure 4.9: SEM micrograph of caprine bone specimens sintered at 1500°C

4.6 Relative density

Due to the rise in sintering temperature, the growth of grain should expect to result in denser specimens generally. Human cortical bone is reported to be having porosity of roughly 30% (Koester, Ager, & Ritchie, 2008). The change in relative density of sintered samples in according to sintering temperature is shown in Fig 4.10. Overall the specimens did increase in relative density when the sintering temperature except some fluctuation in

the higher region. The range of density for bovine and caprine specimens are much smaller as compared to the galline samples.

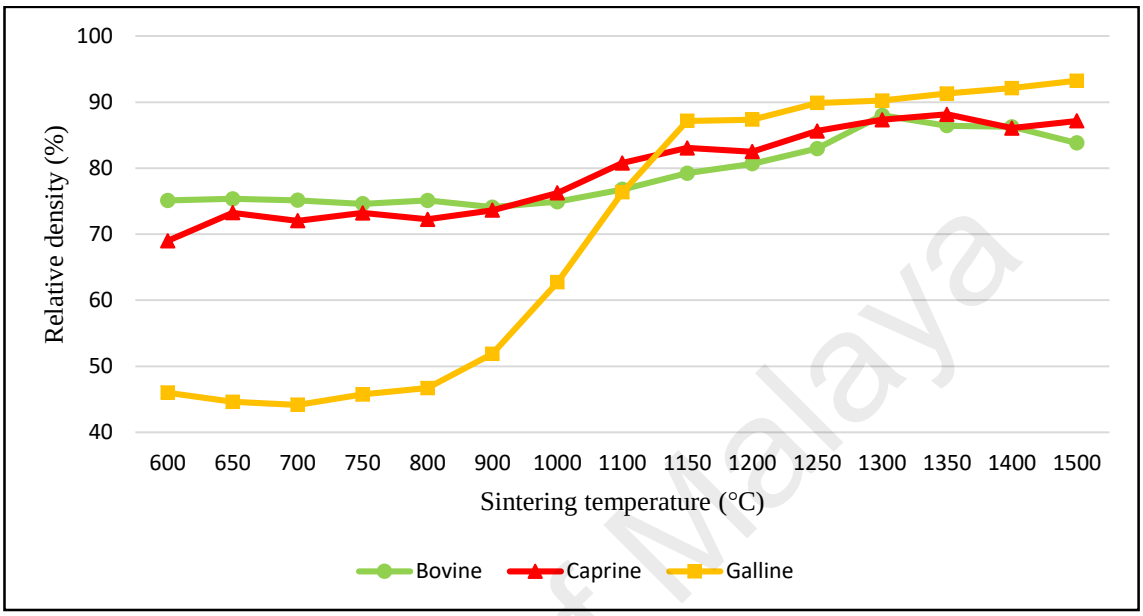

Figure 4.10: Graph of relative density against sintering temperature

When sintered at 600°C, both specimens of bovine and caprine showed relative density of 75.11% and 69.01% which were close to the density of human bone as reported. Although from different species but raw galline bone also having porosity of about 30% but in this study it was only 45.98% after sintered at 600°C (Williams, Waddington, Murray, & Farquharson, 2004). The reason for this observation being the high total amount of organic compounds found in the bone structure burnt off and left a porous structure.

In the case of bovine bone, the specimens showed increasing trend in relative density following the increase in sintering temperature although there are some slight fluctuation. However, the trend reached peak at 1300°C with 88% and then decreased.

When comparing with the changes in XRD pattern, the specimens stayed phase pure HA up till 1300°C and then decomposed into β-TCP followed by α-TCP. The changes in phase were in good agreement with the trend in relative density due to differences in density. The relative density of HA, β-TCP and α-TCP are 3.16 g cm^{-3}, 3.066 g cm^{-3} and 2.866 g cm^{-3}.

Looking at the trend of caprine bone samples, overall it showed increasing trend too with some slight fluctuation in between. Right up to 1100°C, the specimen from caprine bone was still having the highest relative density among the 3 type of bones. The decomposition of phase from HA to β-TCP did not caused drastic effect. The major difference between caprine and bovine was that none of the caprine bone specimens decomposed into α-TCP which having the lowest relative density among 3 phases.

Sintered galline bone specimens showed the largest change among the 3 type of bones. Starting from 45.98% at 600°C, the increasing trend continuously rise to 93.25% at 1500°C. The most significant increase was observed between 900°C to 1150°C. The relative density leaped from 51.87% to 87.16%. The big increment in the relative density was mainly due to the merging of HA particles. The formation of large grain reduced the porosity found in the fibrous network structure. The galline bone specimen sintered at 1500°C attained the highest relative density in this study which was 93.25%.

4.7 Microhardness

Microhardness test was done on the sintered bone specimens. According to study done before, the average Vickers hardness of human Cortical and Cancellous bone were

reported to be 396MPa and 345MPa respectively (Pramanik, Agarwal, Rai, & Garg, 2007). Although there are many anatomical sites of the human skeleton, but study reported that the hardness of bone was depending on the type of tissue instead of anatiomical site (Ohman, Zwierzak, Baleani, & Viceconti, 2013).

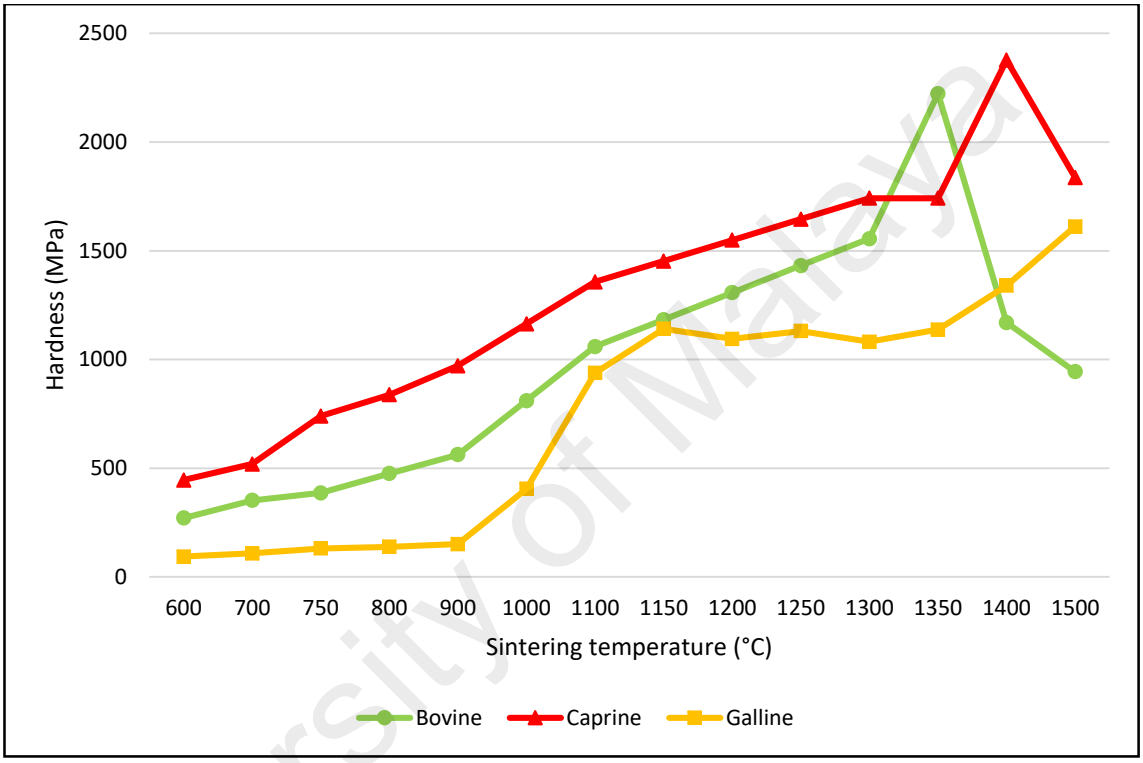

Figure 4.11: Graph of hardness against sintering temperature

Sintered specimens of bovine bone observed to be having medium hardness among the 3 type of bones. Starting from 271.3 MPa at 600°C, the hardness increased in a linear manner to 562.6 MPa at 900°C. At 1300°C, the hardness read 1556 MPa and attained the peak in this study, 2223 MPa at 1350°C. The hardness was there decreased on 1400°C and 1500°C. When cross checking with XRD patterns of bovine bone specimens, the changes in hardness was in agreement. After the peak, the hardness of

specimens decreased by about half to 1170 MPa and 944.4 MPa. This phenomenal was explainable by the properties of phase changing to α-TCP as although it is biocompatible as β-TCP but it is more soluble and biodegradeable (Carrodeguas & De Aza, 2011).

The hardness values for sintering temperature between 1000°C to 1250°C were not available for both bovine and caprine bone specimens because the sintered specimens shattered into small pieces and powdery form after cooling down from sintering process. The specimens were left to cool down in controlled environment to room temperature and hold for at least 12 hours before proceeding to analysis. However, specimens from both bovine and caprine bones showed crack line upon taking from the box furnace and then shattered. After observation of morphology under SEM it was found out that instead of a well structure of grains, the specimens formed small chunks that were not fused together. This is deduced that the specimens were initially only holding the shape due to capillary force.

Observing the overall trend of the hardness of caprine specimens, it can be found that they were the highest among the 3 type of bones at almost every sintering temperature. The hardness of caprine bone specimens followed the trend of bovine bone specimens that increased up till a peak point and then drop down. Started at 445.6 MPa, the hardness increased to 971.5 MPa at 900°C. Then, the hardness remained the same at 1742 MPa for 1300°C and 1350°C. The highest reading in this study among the 3 type of bones were observed at 2377 MPa when the carpine bone specimen sintered at 1400°C. The hardness then dropped slightly to 1837 MPa at 1500°C.

Hardness of galline bone specimens were recorded for full temperature range. Overall, it was an increasing trend with some slight fluctuation between 1150°C to 1350°C. As of observed in the trend of relative density, the hardness of galline bone specimens also increased drastically between the temperature range of 900°C to 1150°C where the grain growth was rapid and particles consolidating. The hardness of galline bone specimens shown lowest of 94.21 MPa at 600°C and increased up to the peak of 1612 MPa at 1500°C. Although the percentage of β-TCP and α-TCP were increasing following the increase in sintering temperature but the grain growth and consolidation process did contribute to the increasing in hardness.

The hardness of sintered bovine bone and caprine bone specimens increased by big amount although the relative density only increased in small amount. The main contribution was the growth of grains network which form strong structure although they did not consolidate as much as observed in galline bone specimens. In agreement with study done previously, the relative density were reported to be 62% to 87% when bovine bone specimens were sintered between 800°C to 1200°C (Yazdanpanah, Bahrololoom, & Hashemi, 2015). Noticeable gain in hardness in relation to the relative density was observed on the galline bone specimens when sintered at increasing sintering temperature.

When looking at the result from both the relative density of sintered samples and hardness of sintered samples, it is able to conclude that on overall the increase in relative density showing direct positive increases in the hardness of the sintered samples. This is due to the growth of the grains making the samples became denser and hence producing samples with higher hardness. The strong particle structure is able to withstand more load.

4.8 Summary

In this chapter, the sintered specimens of bovine, caprine and galline bone at various temperature were compared in terms of phase stability, microstructure, relative density and mechanical strength. In general, the specimens gained well form structure and mechanical strength when the sintering temperature increases but the phase changes. Different type of bone was found to be phase stable up to different temperature point and starts to change in phase.

CHAPTER 5: CONCLUSIONS AND RECOMMENDATIONS

5.1 Conclusions

In this study, bovine, caprine and galline bones were used as the natural raw material for producing HA through heat treatment process. The specimens were heat treated from 600°C up to 1500°C. The specimens were then analysed and studied through several testing processes. The findings of the study were summarized as below:

1. Phase pure HA was able to be produced from raw bone of bovine, caprine and galline through heat treatment process without using chemical substances.
2. When exceeded certain temperature point, the HA will decompose into β-TCP or α-TCP and hence obtained biphasic material.
3. Upon heat treatment process, FTIR spectrum confirmed that all the organic compounds found in the raw bone were removed which would be safe to be used in application of biomedical.
4. By observing the SEM micrographs, it was able to find out that the structure of specimens changed from similar structure of raw bones into fibrous network structure with higher amount of porosity. When the sintering temperature were increased, the specimens started to grow in grains and consolidate.
5. When sintered at temperature between 1000°C and 1250°C, the specimens shattered after cooling down. It was due to that the specimens were only holding the shape by capillary force from the press forming process.
6. Average grain size of specimens were only calculated for sintering temperature of 1350°C, 1400°C and 1500°C due to unclear grain boundary found on specimens sintered at other temperature.
7. The average grain size increased following the increased in sintering temperature. The proportion of increament for bovine and caprine bone

specimens were almost the same at lower amount while the average grain size of galline bone specimens increased rapidly.

8. The average grain size in this study were found to be between 5.367 μm to 35.57 μm.
9. Range of relative density in this study range from 44.14% for galline bone sintered at 700°C up to 93.25% also for galline bone but sintered at 1500°C. The minimum and maximum changes in relative density for bovine bone was 13.92%, 19.14% for caprine bone and 49.11% for galline bone.
10. The large changes in relative density of galline bone as opposed to the bovine and caprine bone is due to the high total amount of protein found in the galline bone which they were burnt off easily during heat treatment leaving high porosity structure. The harness of the HA sample increases proportionally with the increase in relative density.
11. Hardness for sintered specimens in this study found to be ranged between 94.21 MPa from galline bone sintered at 600°C and as high as 2377 MPa when the caprine bone was sintered at 1400°C. In comparison, the average hardness of human bone was found to be 396MPa and 345MPa for Cortical and Cancellous bone respectively.
12. The hardness for bovine and caprine hitted peak before the highest sintering temperature in this study and showed downwards trend while the galline bone was in increasing trend up to highest sintering temperature.
13. Concluding from this study, it is able to produce sintered specimen from raw bovine, caprine or galline bones with various characteristics and mechanical properties through controlled sintering temperature.

5.2 Recommendations for future work

The following suggestions were made for further study in producing HA from natural raw animal bones:

1. Further increase the sintering temperature as when hitting the maximum sintering temperature in this study, some of the specimens were still showing increasing trend in mechanical properties.
2. More varieties of animal bones.
3. Mixture of animal bones in a single specimens due to as what found out in this study, each type of animal bones was showing different behaviours when treated at various temperature.
4. Other sintering techniques could be adopted such as microwave and plasma sintering as the rapid growth in fine grain could produce specimens which are translucent as reported in study done previously.
5. In vitro study should be carried out to further investigate the biological properties of sintered specimens of different type of animal bones.

REFERENCES

Aerssens, J., Boonen, S., Lowet, G., & Dequeker, J. (1998). Interspecies differences in bone composition, density, and quality: potential implications for in vivo bone research. *Endocrinology, 139*(2), 663-670. doi:10.1210/endo.139.2.5751

Al-Weshahy, A., & Venket Rao, A. (2009). Isolation and characterization of functional components from peel samples of six potatoes varieties growing in Ontario. *Food Research International, 42*(8), 1062-1066. doi:http://dx.doi.org/10.1016/j.foodres.2009.05.011

Alexander C. Allori, Alexander M. Sailon, & Stephen M. Warren. (2008). Biological Basis of Bone Formation, Remodeling, and Repair - Part I: Biochemical Signaling Molecules. *Tissue Engineering Part B: Reviews, 14*(3), 259-273.

ASM International, H. C. (1991). *Ceramics and Glasses* (Vol. 4): ASM International.

ASTM. (2004). E112-96 *Standard Test Methods for Determining Average Grain Size*. West Conshohocken, PA: ASTM.

Benmarouane, A., Hansen, T., & Lodini, A. (2004). Heat treatment of bovine bone preceding spatially resolved texture investigation by neutron diffraction. *Physica B: Condensed Matter, 350*(1-3), E611-E614.

Bigi, A., Boanini, E., & Gazzano, M. (2016). 7 - Ion substitution in biological and synthetic apatites A2 - Aparicio, Conrado. In M.-P. Ginebra (Ed.), *Biomineralization and Biomaterials* (pp. 235-266). Boston: Woodhead Publishing.

Boutinguiza, M., Pou, J., Comesana, R., Lusquinos, F., Carlos, A. d., & Leon, B. (2012). Biological hydroxyapatite obtained from fish bones. *Materials Science and Engineering C, 32*, 478-486.

Carrodeguas, R. G., & De Aza, S. (2011). α-Tricalcium phosphate: Synthesis, properties and biomedical applications. *Acta Biomaterialia, 7*(10), 3536-3546. doi:http://dx.doi.org/10.1016/j.actbio.2011.06.019

Chen, Q., & Thouas, G. A. (2015). Metallic implant biomaterials. *Materials Science and Engineering: R: Reports, 87*, 1-57. doi:https://doi.org/10.1016/j.mser.2014.10.001

Corno, M., Busco, C., Civalleri, B., & Ugliengo, P. (2006). Periodic ab initio study of structural and vibrational features of hexagonal hydroxyapatite Ca10(PO4)6(OH)2. *Phys Chem Chem Phys, 8*(21), 2464-2472. doi:10.1039/b602419j

Currey, J. D., Brear, K., & Zioupos, P. (1996). The effects of ageing and changes in mineral content in degrading the toughness of human femora. *Journal of Biomechanics, 29*(2), 257-260.

Danilchenko, S. N., Koropov, A. V., Protsenko, I. Y., Sulkio-Cleff, B., & Sukhodub, L. F. (2006). Thermal behavior of biogenic apatite crystals in bone: An X-ray

diffraction study. *Crystal Research and Technology, 41*(3), 268-275. doi:10.1002/crat.200510572

Dorozhkin, S. V. (2010). Calcium Orthophosphates as Bioceramics: State of the Art. *Journal of Functional Biomaterials, 1*(1), 22-107.

Fernandez, E., Gil, F. J., Ginebra, M. P., Driessens, F. C., Planell, J. A., & Best, S. M. (1999). Calcium phosphate bone cements for clinical applications. Part I: solution chemistry. *J Mater Sci Mater Med, 10*(3), 169-176.

Figueiredo, M., Fernando, A., Martins, G., Freitas, J., Judas, F., & Figueiredo, H. (2010). Effect of the calcination temperature on the composition and microstructure of hydroxyapatite derived from human and animal bone. *Ceramics International, 36*(8), 2383-2393. doi:10.1016/j.ceramint.2010.07.016

Fuh, L.-J., Huang, Y.-J., Chen, W.-C., & Lin, D.-J. (2017). Preparation of micro-porous bioceramic containing silicon-substituted hydroxyapatite and beta-tricalcium phosphate. *Materials Science and Engineering: C, 75*, 798-806. doi:https://doi.org/10.1016/j.msec.2017.02.065

Galambos, M., Suchanek, P., & Rosskopfova, O. (2012). Sorption of anthropogenic radionuclides on natural and synthetic inorganic sorbents. *Journal of Radioanalytical and Nuclear Chemistry, 293*(2), 613-633.

Gerhard Meisenberg, & Willian H. Simmons. (2011). *Principles of Medical Biochemistry*: Elsevier Health Sciences.

Ghiasi, M. S., Chen, J., Vaziri, A., Rodriguez, E. K., & Nazarian, A. (2017). Bone fracture healing in mechanobiological modeling: A review of principles and methods. *Bone Rep, 6*, 87-100. doi:10.1016/j.bonr.2017.03.002

Goto, T., & Sasaki, K. (2014). Effects of trace elements in fish bones on crystal characteristics of hydroxyapatite obtained by calcination. *Ceramics International, 40*, 10777-10785.

Haberko, K., Bućko, M. M., Brzezińska-Miecznik, J., Haberko, M., Mozgawa, W., Panz, T., . . . Zarębski, J. (2006). Natural hydroxyapatite—its behaviour during heat treatment. *Journal of the European Ceramic Society, 26*(4–5), 537-542. doi:http://dx.doi.org/10.1016/j.jeurceramsoc.2005.07.033

Ho, W.-F., Hsu, H.-C., Hsu, S.-K., Hung, C.-W., & Wu, S.-C. (2013). Calcium phosphate bioceramics synthesized from eggshell powders through a solid state reaction. *Ceramics International, 39*(6), 6467-6473. doi:http://dx.doi.org/10.1016/j.ceramint.2013.01.076

J. A. Buckwalter, R. R. Cooper, M. J. Flimcher, & Recker, R. (1995). Bone Biology - Part II: Formation, Form, Modeling, Remodeling and Regulation of Cell Function. *The Journal of Bone & Joint Surgery, 77-A*, 1276-1289.

Janus, A. M., Faryna, M., Haberko, K., Rakowska, A., & Panz, T. (2008). Chemical and micrstructural characterization of natural hydroxyapatite derived from pig bones. *Microchimica Acta, 161*, 349-353.

Ji, B. H., & Gao, H. J. (2004). Mechanical properties of nanostructure of biological materials. *Journal of the Mechanics and Physics of Solids, 52*(9), 1963-1990.

Jinlong, N., Zhenxi, Z., & Dazong, J. (2001). Investigation of Phase Evolution During the Thermochemical Synthesis of Tricalcium Phosphate. *Journal of Materials Synthesis and Processing, 9*(5), 235-240. doi:10.1023/a:1015243216516

Juang, H. Y., & Hon, M. H. (1996). Effect of calcination on sintering of hydroxyapatite. *Biomaterials, 17*(21), 2059-2064.

Kalfas, I. H. (2001). Principles of bone healing. *Neurosurg Focus, 10*(4).

Kamalanathan, P., Ramesh, S., Bang, L. T., Niakan, A., Tan, C. Y., Purbolaksono, J., . . . Teng, W. D. (2014). Synthesis and sintering of hydroxyapatite derived from eggshells as a calcium precursor. *Ceramics International, 40*(10), 16349-16359. doi:DOI 10.1016/j.ceramint.2014.07.074

Khan, Y. M., Katti, D. S., & Laurencin, C. T. (2004). Novel polymer-synthesized ceramic composite-based system for bone repair: an in vitro evaluation. *J Biomed Mater Res A, 69*(4), 728-737. doi:10.1002/jbm.a.30051

Kim, S., Kong, Y. M., Lee, I. S., & Kim, H. E. (2002). Effect of calcinations of starting powder on mechanical properties of hydroxyapatite-alumina bioceramic composite. *J Mater Sci Mater Med, 13*(3), 307-310.

Koester, K. J., Ager, J. W., & Ritchie, R. O. (2008). The true toughness of human cortical bone measured with realistically short cracks. *Nat Mater, 7*(8), 672-677. doi:http://www.nature.com/nmat/journal/v7/n8/suppinfo/nmat2221_S1.html

Koutsopoulos, S. (2002). Synthesis and characterization of hydroxyapatite crystals: a review study on the analytical methods. *J Biomed Mater Res, 62*(4), 600-612. doi:10.1002/jbm.10280

Kumta, P. N., Sfeir, C., Lee, D. H., Olton, D., & Choi, D. (2005). Nanostructured calcium phosphates for biomedical applications: novel synthesis and characterization. *Acta Biomaterialia, 1*(1), 65-83. doi:DOI 10.1016/j.actbio.2004.09.008

Leventouri, T. (2006). Synthetic and biological hydroxyapatites: crystal structure questions. *Biomaterials, 27*(18), 3339-3342.

Li, Y., & Aparicio, C. (2013). Discerning the Subfibrillar Structure of Mineralized Collagen Fibrils: A Model for the Ultrastructure of Bone. *PLOS ONE, 8*(9), e76782. doi:10.1371/journal.pone.0076782

Lin, X., Yang, S., Lai, K., Yang, H., Webster, T. J., & Yang, L. (2017). Orthopedic implant biomaterials with both osteogenic and anti-infection capacities and associated in vivo evaluation methods. *Nanomedicine: Nanotechnology, Biology and Medicine, 13*(1), 123-142. doi:https://doi.org/10.1016/j.nano.2016.08.003

Lorprayoon, C. (1989). Synthesis of calcium hydroxyapatite and tricalcium phosphate from bone ash. *Ion. Polym. Order. Polym. Hi. Perf. Mater. Biomater*, 329-336.

Mendelson, M. I. (1969). Average Grain Size in Polycrystalline Ceramics. *Journal of the American Ceramic Society, 52*(8), 443-446. doi:10.1111/j.1151-2916.1969.tb11975.x

Mucalo, M. R. (2015). 14 - Animal-bone derived hydroxyapatite in biomedical applications. In M. Mucalo (Ed.), *Hydroxyapatite (Hap) for Biomedical Applications* (pp. 307-342): Woodhead Publishing.

N. Umadevi, & Dr. S.N. Geethalakshmi. (2011). A brief study on human bone anatomy and bone fractures. *International Journal of Computer Engineering Science, 1*(3).

Negro, C., Tommasi, L., & Miceli, A. (2003). Phenolic compounds and antioxidant activity from red grape marc extracts. *Bioresource Technology, 87*(1), 41-44. doi:Pii S0960-8524(02)00202-X

Doi 10.1016/S0960-8524(02)00202-X

Niakan, A., Ramesh, S., Ganesan, P., Tan, C. Y., Purbolaksono, J., Chandran, H., . . . Teng, W. D. (2014). Sintering behaviour of natural porous hydroxyapatite derived from bovine bone. *Ceramics International*.

Ofudje, E. A., Rajendran, A., Adeogun, A. I., Idowu, M. A., Kareem, S. O., & Pattanayak, D. K. (2018). Synthesis of organic derived hydroxyapatite scaffold from pig bone waste for tissue engineering applications. *Advanced Powder Technology*, *29*(1), 1-8. doi:https://doi.org/10.1016/j.apt.2017.09.008

Ohman, C., Zwierzak, I., Baleani, M., & Viceconti, M. (2013). Human bone hardness seems to depend on tissue type but not on anatomical site in the long bones of an old subject. *Proc Inst Mech Eng H, 227*(2), 200-206. doi:10.1177/0954411912459424

Ooi, C. Y., Hamdi, M., & Ramesh, S. (2007). Properties of hydroxyapatite produced by annealing of bovine bone. *Ceramics International, 33*(7), 1171-1177.

Ozyegin, L. S., Oktar, F. N., Goller, G., Kayali, E. S., & Yazici, T. (2004). Plasma-sprayed bovine hydroxyapatite coatings. *Materials Letters, 58*(21), 2605-2609.

Palanivelu, R., Saral, A. M., & Kumar, A. R. (2014). Nanocrystalline hydroxyapatite prepared under various pH conditions. *Spectrochimica Acta Part A: Molecular and Biomolecular Spectroscopy, 131*, 37-41.

Palazzo, B., Iafisco, M., Laforgia, M., Margiotta, N., Natile, G., Bianchi, C. L., . . . Roveri, N. (2007). Biomimetic hydroxyapatite-drug nanocrystals as potential bone substitutes with antitumor drug delivery properties. *Advanced Functional Materials, 17*(13), 2180-2188. doi:10.1002/adfm.200600361

Palmer, L. C., Newcomb, C. J., Kaltz, S. R., Spoerke, E. D., & Stupp, S. I. (2008). Biomimetic Systems for Hydroxyapatite Mineralization Inspired By Bone and Enamel. *Chemical Reviews, 108*(11), 4754-4783. doi:10.1021/cr8004422

Patil, A. S., Sable, R. B., & Kothari, R. M. (2011). An update on transforming growth factor-beta (TGF-beta): sources, types, functions and clinical applicability for cartilage/bone healing. *J Cell Physiol, 226*(12), 3094-3103. doi:10.1002/jcp.22698

Pramanik, S., Agarwal, A. K., Rai, K. N., & Garg, A. (2007). Development of high strength hydroxyapatite by solid-state-sintering process. *Ceramics International, 33*(3), 419-426. doi:http://dx.doi.org/10.1016/j.ceramint.2005.10.025

R. Murugan, & S. Ramakrishna. (2005). Development of nanocomposites for bone grafting. *Composites Science and Technology, 65*, 2385-2406.

Ramesh, S. (2001). Grain size-properties correlation in polycrystalline hydroxyapatite bioceramic. *Malaysian Journal of Chemistry, 3*, 35-40.

Rao, R. R., & Kannan, T. S. (2002). Synthesis and sintering of hydroxyapatite-zirconia composites. *Materials Science & Engineering C-Biomimetic and Supramolecular Systems, 20*(1-2), 187-193.

Rheumatology, A. C. o. (2009). Bone Architecture *http://images.rheumatology.org/viewphoto.php?imageId=2861777* (Vol. 99-15-0018, pp. Bone is comprised of two subtypes: cortical (compact) and trabecular (cancellous). Cortical bone has higher density and is the major structural component. Trabecular bone has a greater surface area and is more metabolically active. The hip contains both types of bone; however, the predominant component is cortical. Long (appendicular) bones such as the hip and radius are predominantly cortical in nature, whereas the spine (axial bone) is largely trabecular.). Rheumatology Image Library: American College of Rheumatology.

Rho, J.-Y., Kuhn-Spearing, L., & Zioupos, P. (1998). Mechanical properties and the hierarchical structure of bone. *Medical Engineering & Physics, 20*, 92-102.

Ribeiro, M., Fraguas, E. H., Brito, K. I. C., Kim, Y. J., Pallos, D., & Sendyk, W. R. (2018). Bone autografts & allografts placed simultaneously with dental implants in rabbits. *Journal of Cranio-Maxillofacial Surgery, 46*(1), 142-147. doi:https://doi.org/10.1016/j.jcms.2017.11.006

Rujitanapanich, S., Kumpapan, P., & Wanjanoi, P. (2014). Synthesis of Hydroxyapatite from Oyster Shell via Precipitation. *11th Eco-Energy and Materials Science and Engineering (11th Emses), 56*, 112-117. doi:10.1016/j.egypro.2014.07.138

Ruksudjarit, A., Pengpat, K., Rujijanagul, G., & Tunkasiri, T. (2008). Synthesis and characterization of nanocrystalline hydroxyapatite from natural bovine bone. *Current Applied Physics, 8*(3-4), 270-272.

S. N. Danilchenko, A. V. Koropov, I .Yu. Protsenko, B. Sulkio-Cleff, & Sukhodub, L. F. (2006). Thermal behavior of biogenic apatite crystals in bone: An X-ray diffraction study. *Crystal Research and Technology*, *41*(3), 268-275.

S. Viguet-Carrin, P. Garnero, & P.D. Delmas. (2005). The role of collagen in bone strength. *Osteoporos International, 2016*(17), 319-336. doi:10.1007/s00198-005-2035-9

S. Weiner, & H. D. Wagner. (1998). THE MATERIAL BONE: Structure-Mechanical Function Relations. *Annual Review of Materials Science, 28*, 271-298. doi:10.1146/annurev.matsci.28.1.271

Sansalone, V., Naili, S., Bousson, V., Bergot, C., Peyrin, F., Zarka, J., . . . Haiat, G. (2010). Determination of the heterogeneous anisotropic elastic properties of human femoral bone: from nanoscopic to organ scale. *J Biomech, 43*(10), 1857-1863. doi:10.1016/j.jbiomech.2010.03.034

Senevirathne, M., Jeon, Y.-J., Ha, J.-H., & Kim, S.-H. (2009). Effective drying of citrus by-product by high speed drying: A novel drying technique and their antioxidant activity. *Journal of Food Engineering, 92*(2), 157-163. doi:http://dx.doi.org/10.1016/j.jfoodeng.2008.10.033

Shi, P., Liu, M., Fan, F., Yu, C., Lu, W., & Du, M. (2018). Characterization of natural hydroxyapatite originated from fish bone and its biocompatibility with osteoblasts. *Materials Science and Engineering: C, 90*, 706-712. doi:https://doi.org/10.1016/j.msec.2018.04.026

Silva, R. V., Bertan, C. A., & Moreira, N. H. (2005). The use of hydroxyapatite and autogenous cancellous bone grafts to repair bone defects in rats. *International Journal of Oral & Maxillofacial Surgery*, *34*(2), 178-184.

Sobczak-Kupiec, A., & Wzorek, Z. (2012). The influence of calcination parameters on free calcium oxide content in natural hydroxyapatite. *Ceramics International, 38*, 641-647.

Sopyan, I., & Kaur, J. (2009). Preparation and characterization of porous hydroxyapatite through polymeric sponge method. *Ceramics International, 35*(8), 3161-3168. doi:http://dx.doi.org/10.1016/j.ceramint.2009.05.012

Suchanek, W. L., Shuk, P., Byrappa, K., Riman, R. E., TenHuisen, K. S., & Janas, V. F. (2002). Mechanochemical–hydrothermal synthesis of carbonated apatite powders at room temperature. *Biomaterials, 23*(3), 699-710. doi:http://dx.doi.org/10.1016/S0142-9612(01)00158-2

Sung, Y.-M., Lee, J.-C., & Yang, J.-W. (2004). Crystallization and sintering characteristics of chemically precipitated hydroxyapatite nanopowder. *Journal of Crystal Growth, 262*(1–4), 467-472. doi:http://dx.doi.org/10.1016/j.jcrysgro.2003.10.001

Van Lierde, C., Depreitere, B., Vander Sloten, J., Van Auderkercke, R., Van Der Perre, G., & Goffin, J. (2003). Skull biomechanics: The energy absorbability of the

human skull frontal bone during fracture under quasi-static loading. *J Appl Biomater Biomech, 1*(3), 194-199.

Viswanath, B., & Ravishankar, N. (2008). Controlled synthesis of plate-shaped hydroxyapatite and implications for the morphology of the apatite phase in bone. *Biomaterials, 29*(36), 4855-4863. doi:DOI 10.1016/j.biomaterials.2008.09.001

Walters, M. A., Leung, Y. C., Blumenthal, N. C., LeGeros, R. Z., & Konsker, K. A. (1990). A Raman and infrared spectroscopic investigation of biological hydroxyapatite. *J Inorg Biochem, 39*(3), 193-200.

Wang, L. J., & Nancollas, G. H. (2008). Calcium Orthophosphates: Crystallization and Dissolution. *Chemical Reviews, 108*(11), 4628-4669. doi:DOI 10.1021/cr0782574

Williams, B., Waddington, D., Murray, D. H., & Farquharson, C. (2004). Bone strength during growth: influence of growth rate on cortical porosity and mineralization. *Calcif Tissue Int, 74*(3), 236-245. doi:10.1007/s00223-002-2124-0

Wu, S. C., Tsou, H. K., Hsu, H. C., Hsu, S. K., Liou, S. P., & Ho, W. F. (2013). A hydrothermal synthesis of eggshell and fruit waste extract to produce nanosized hydroxyapatite. *Ceramics International, 39*(7), 8183-8188. doi:DOI 10.1016/j.ceramint.2013.03.094

Xue-Nan Gu, & Yu-Feng Zheng. (2010). A review on magnesium alloys as biodegradable materials. *Front. Mater. Sci. China, 4*(2), 111-115.

Yamada, M., & Egusa, H. (2018). Current bone substitutes for implant dentistry. *Journal of Prosthodontic Research, 62*(2), 152-161. doi:https://doi.org/10.1016/j.jpor.2017.08.010

Yazdanpanah, Z., Bahrololoom, M. E., & Hashemi, B. (2015). Evaluating morphology and mechanical properties of glass-reinforced natural hydroxyapatite composites. *J Mech Behav Biomed Mater, 41*, 36-42. doi:10.1016/j.jmbbm.2014.09.021

Yetmez, M., Erkmen, Z. E., Kalkandelen, C., Ficai, A., & Oktar, F. N. (2017). Sintering effects of mullite-doping on mechanical properties of bovine hydroxyapatite. *Materials Science and Engineering: C, 77*, 470-475. doi:https://doi.org/10.1016/j.msec.2017.03.290

Yoganang, C. P., Selvarajan, V., Wu, J., & Xue, D. Processing of bovine hydroxyapatite powders and synthesis of calcium phosphate silicate glass ceramics.

Younesi, M., Javadpour, S., & Bahrololoom, M. E. (2011). Effect of Heat Treatment Temperature on Chemical Compositions of Extracted Hydroxyapatite from Bovine Bone Ash. *Journal of Materials Engineering and Performance, 20*(8), 1484-1490.

Zhang, J., Xiao, D., He, X., Shi, F., Luo, P., Zhi, W., . . . Weng, J. (2018). A novel porous bioceramic scaffold by accumulating hydroxyapatite spheres for large bone tissue engineering. III: Characterization of porous structure. *Materials Science and Engineering: C, 89*, 223-229. doi:https://doi.org/10.1016/j.msec.2018.04.013

LIST OF PUBLICATIONS AND PAPER PRESENTED

1. S. Ramesh, Z.Z. Loo, C.Y. Tan, W.J. Kelvin Chew, Y.C. Ching, F. Tarlochan, Hari Chandran, S. Krishnasamy, L.T. Bang and Ahmed A.D. Sarhan (2018). Characterization of biogenic hydroxyapatite derived from animal bones for biomedical applications. *Ceramics International*, *44*(9), 505-510. Doi: 10.1016/j.ceramint.2018.03.072

2. Awarded Golden Medal for "Characterisation of hydroxyapatite derived from animal bones" at International Scientific Season for Conferences, Workshops and Training Institutions Exhibition, Kuala Lumpur, Malaysia, 2015.